EvoDevo

RESEARCH Open Access

Shared regulatory function of non-genomic thyroid hormone signaling in echinoderm skeletogenesis

Elias Taylor[1*], Megan Corsini[1] and Andreas Heyland[1]

Abstract

Thyroid hormones are crucial regulators of metamorphosis and development in bilaterians, particularly in chordate deuterostomes. Recent evidence suggests a role for thyroid hormone signaling, principally via 3,5,3′,5′-Tetraiodo-L-thyronine (T4), in the regulation of metamorphosis, programmed cell death and skeletogenesis in echinoids (sea urchins and sand dollars) and sea stars. Here, we test whether TH signaling in skeletogenesis is a shared trait of Echinozoa (Echinoida and Holothouroida) and Asterozoa (Ophiourida and Asteroida). We demonstrate dramatic acceleration of skeletogenesis after TH treatment in three classes of echinoderms: sea urchins, sea stars, and brittle stars (echinoids, asteroids, and ophiuroids). Fluorescently labeled thyroid hormone analogues reveal thyroid hormone binding to cells proximal to regions of skeletogenesis in the gut and juvenile rudiment. We also identify, for the first time, a potential source of thyroxine during gastrulation in sea urchin embryos. Thyroxine-positive cells are present in tip of the archenteron. In addition, we detect thyroid hormone binding to the cell membrane and nucleus during metamorphic development in echinoderms. Immunohistochemistry of phosphorylated MAPK in the presence and absence of TH-binding inhibitors suggests that THs may act via phosphorylation of MAPK (ERK1/2) to accelerate initiation of skeletogenesis in the three echinoderm groups. Together, these results indicate that TH regulation of mesenchyme cell activity via integrin-mediated MAPK signaling may be a conserved mechanism for the regulation of skeletogenesis in echinoderm development. In addition, TH action via a nuclear thyroid hormone receptor may regulate metamorphic development. Our findings shed light on potentially ancient pathways of thyroid hormone activity in echinoids, ophiuroids, and asteroids, or on a signaling system that has been repeatedly co-opted to coordinate metamorphic development in bilaterians.

Introduction

Thyroid hormones (THs) regulate metamorphosis, skeletogenesis, and diverse physiological/developmental systems in chordate deuterostomes. Evidence also suggests a role for TH signaling in non-chordate bilaterians [11, 15, 29, 44, 47, 90, 91, 103, 106]. Thyroxine (T4) is the most abundant TH analogue in nature. Many non-bilaterians use THs and other iodinated tyrosine derivatives as structural elements or to scavenge free radicals (reviewed in [103]). T4 is the typical first step in TH synthesis [29, 30, 82, 87, 94, 103], a biochemical process predating metazoans [42, 82, 103]. Therefore, the use of THs as a signaling agent to regulate development and metamorphosis can be considered a derived trait of some metazoans.

L-Triiodothyronine (T3), a metabolite of T4 and active hormone in vertebrates, has been shown to regulate development and metamorphosis [8], with T4 acting synergistically via binding to an integrin membrane receptor [22, 25]. In contrast, T4 has roughly ten-fold

*Correspondence:
Elias Taylor
elias@uoguelph.ca
[1] College of Biological Sciences, University of Guelph, Integrative Biology, Guelph, ON N1G-2W1, Canada

greater efficacy than T3 on regulation of development, settlement, and metamorphosis in some non-chordates, including sea urchins and molluscs [15, 49, 103, 106].

There are three major categories of mechanism by which thyroid hormone signal transduction occurs: (1) genomic signaling, defined as TH signaling via a nuclear hormone receptor bound to the genome [7, 103], (2) extra-nuclear actions of a nuclear hormone receptor [25, 105] and (3) integrin-mediated MAPK phosphorylation cascade [25, 103]. The specific mechanisms governing TH actions in non-chordates remain largely unknown, despite new insights from echinoderms, mollusks, and cnidarians. Two main TH receptors, the nuclear thyroid hormone receptor (THR) and RGD-binding integrins, are common to all bilaterians and all metazoans, respectively [103, 105]. In vertebrates, RGD competition with T4 at integrin αVβ3 is well established [3, 17, 18, 24, 26, 50, 61, 63]. It has been previously established in sea urchins that RGD peptide is a competitive ligand at a membrane receptor [104]. T4 has been shown to accelerate metamorphic development in echinoderms and molluscs [10, 15, 36, 43, 44, 46, 53, 54, 91]. Evidence suggests that these mechanisms may rely on the nuclear hormone receptor-mediated pathway [49, 106] and that THR may regulate apoptosis and skeletogenesis in sea urchins [106, 113]. In addition, embryonic and larval sea urchin skeletogenesis may be regulated by the TH-integrin-mediated pathway [104].

Taylor and Heyland [103] suggested that sea urchin skeletogenesis is regulated by thyroid hormones via a non-genomic integrin-mediated MAPK cascade triggered by direct TH binding to skeletogenic mesenchyme cells. In addition, Wynen et al. [113] demonstrated a role for THs regulating apoptosis in metamorphic development. Thyroid hormones have been shown to be synthesized by sea urchin embryos and larvae [15, 44]. Uptake mechanisms have been previously characterized [74] and involve peroxidase-facilitated diffusion coupled with iodination of tyrosines in sea urchins. However, the source of THs and the location of TH receptors are unclear, and it is unknown if TH signaling and its involvement in skeletogenesis is limited to S. purpuratus larvae, or if it can be generalized to other sea urchins and echinoderms.

Indirect-developing echinoderms are characterized by a biphasic life cycle with a planktonic phase followed by settlement to the benthos and metamorphosis. Sea urchin, brittle star, and sea star development to settlement involves the production of juvenile structures in the pre-settlement larva, including skeletal elements (e.g., skeletal plates, spines, test, and tube-foot rings in sea urchins). The actions of thyroid hormones on skeletogenesis in sea urchins have been of particular interest, as sea urchin larval skeletogenesis is a thoroughly studied model system [93]. In particular, the gene regulatory network (and transcription factors regulating skeletogenesis) has been characterized (e.g., [23, 65, 68, 72, 85]).

In this manuscript, we distinguish between adult and larval skeletogenesis. Adult skeletogenesis begins during metamorphic development in sea urchins, sea stars, and brittle stars. We contrast this with larval skeletogenesis which is a feature of sea urchins and brittle stars, and begins during embryogenesis with additional skeletogenesis during larval development as plutei develop additional pairs of larval arms. In sea urchins, some minor differences in the gene regulatory network governing larval and adult skeletogenesis have been described [37] with adult skeletogenic cells not appearing to arise from the PMC cell lineage, but rather possibly from secondary mesenchyme cells (SMCs; [114]). As well, some larval skeletogenic cells post-embryonic development derive from SMC populations [114] (Fig. 1).

The development of adult skeleton in a coelom or rudiment adjacent to the gut appears to be an ancient

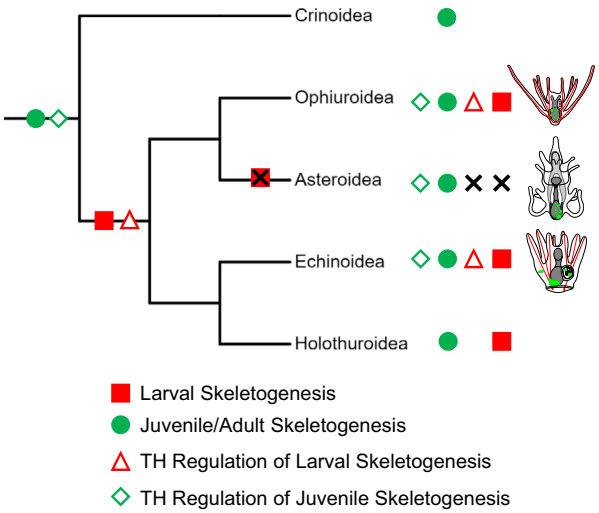

Fig. 1 Hypotheses about the evolution of skeletogenesis across echinoderm taxa with a possible ancestral function of non-genomic thyroid hormone signaling. Recent evidence suggests a single origin of larval skeletogenesis followed by loss in Asteroids (sea stars; [32]), although independent origins of larval skeletogenesis in Ophiuroids (brittle stars) and Echinoids/Holothuroids (sea urchins/sea cucumbers) have also been proposed [12, 28, 70]. We test the hypothesis that THs, predominantly T4, regulate skeletogenesis in Ophiuroids, Echinoids, and Asteroids, as a result of evolutionarily ancient regulation of skeletogenesis by THs. We suggest that TH regulation was co-opted to regulate larval skeletogenesis when the gene regulatory apparatus allowing for skeletogenesis in adults became expressed and co-opted by the larval stage of some echinoderms

and conserved component of echinoderm development [51, 75] and is considered a shared characteristic of all extant echinoderms. In contrast, larval skeletogenesis is likely a synapomorphy of holothuroids (sea cucumbers), echinoids (sea urchins), and ophiuroids (brittle stars) [32]. Crinoids (sea lilies) and asteroids (sea stars) do not feature larval skeletogenesis [93]. Here, we use "adult skeletogenesis" to refer to the development of skeletal elements slated to be incorporated into the juvenile echinoderm, post-settlement (Fig. 2). This skeletal development begins prior to settlement, during metamorphic development when skeleton is deposited by a population of mesenchyme cells with a distinct but similar gene regulatory network to the primary mesenchyme cells (PMCs) responsible for larval skeleton [37, 93, 114]. For instance, sea urchins develop spines, portions of the adult test, and skeletal rings supporting the tube feet [41]. Much of this development occurs in the juvenile rudiment, a structure adjacent to the larval gut which contains most tissues of the developing juvenile echinoderm. Similarly, the larval ophiuroid, asteroid, and holothuroid produce extensive skeleton prior to metamorphosis, mainly in the juvenile rudiment. In Crinoids, an outgroup to the other extant echinoderms, the skeletonized stalk develops from a coelom adjacent to the gut, while the calyx (analogous to the echinoid test), begins developing from extra-coelomic spicules.

In many echinoids and ophiuroids, larval skeleton supports the larval arms, important structures for feeding and defense. During embryonic development, either during gastrulation or immediately following gastrulation, these echinoids and ophiuroids develop larval skeleton from a population of mesenchyme cells separate from the adult/late mesenchymal cells. In holothuroids and ophiuroids, these cells derive from the tip of the archenteron or adjacent coeloms. In echinoids, the PMCs arise from small micromeres at the vegetal pole. From there, the cells migrate to the ventrolateral cluster and form the larval arms in echinoids and ophiuroids. The GRN governing skeletogenesis in these cells is distinct, although it shares a reliance on expression of alx1 and ets1, two key transcription factors in the skeletogenic GRN. Asteroid mesenchymal cells do not express alx1 until expansion of the coeloms prior to rudiment development, likely accounting for the potential loss of skeletogenesis in larval asteroids [59]. Larval skeletogenesis in ophiuroids, echinoids, and holothuroids is a result of a similar GRN to the adult skeletogenic GRN being expressed early in development by mesenchyme cells arising during gastrulation [37].

There are two hypotheses of the origin of larval skeletogenesis; the first posits a single origin of adult skeletogenesis followed by multiple origins of larval skeletogenesis and convergent evolution of larval skeleton. This is owing to the phylogenetic placement of ophiuroids (which produce larval skeleton) as sister group to asteroids (which do not), as well as dissimilarities in the ophiuroid and echinoid larval GRN. The second hypothesis suggests that regardless of the sometimes contentious phylogenetic placement of ophiuroids [9, 84, 86, 107], a single origin of larval skeletogenesis is more likely [32], followed by a potential secondary loss of larval skeleton in asteroidea. Echinoderm skeletogenic GRNs share specific characteristics, such as a conserved role for alx1, ets1, and vegfr, suggesting that differences in echinoid larval skeletogenesis and cell specification may be derived traits [28, 32, 70]. Both hypotheses indicate that adult skeletogenesis arose first, with a single origin. Given the shared origin of larval and adult skeletogenesis in echinoderms, and thyroid hormone regulation of larval and adult skeletogenesis in sea urchins [104, 106], we predict that TH regulation of skeletogenesis would be a shared feature of both larval and adult skeletogenesis in echinoids, ophiuroids, and asteroids.

In this study, we seek to answer the question of whether thyroid hormones accelerate early and late skeletogenesis in two distantly related Echinoderms: the sea star *P. ochraceus*, and the brittle star *O. aculeata*, as well as to confirm previous results showing that thyroid hormones accelerate initiation of skeletogenesis in echinoids. We show that THs are capable of accelerating skeletogenesis in three classes of echinoderms, sea urchins, sea stars, and brittle stars (echinoids, asteroids, and ophiuroids). THs bind to cells proximal to sites of skeletogenesis and induce MAPK phosphorylation and skeletogenesis. These processes can be fully or partially inhibited by a competitive ligand of RGD-binding integrins, and by an inhibitor of MAPK activity. We discuss our findings in the context of the origin and evolution of TH regulation and the evolution of skeletogenesis in echinoderms.

Methods

Animal care

Ophiopholis aculeata were collected in Cobscook Bay, Maine, and shipped to Williamsburg, VA to be spawned (2020–2021). Embryos were shipped overnight on ice to the University of Guelph (ON, Canada) as fertilized eggs in the case of experiments on gastrulae, or 6 days post-fertilization (dpf) in the case of the late-larval experiments. On arrival, ophiuroid larvae were transferred to 2 L beakers at a density of 0.5–1 larva/mL. The cultures were cleaned manually and had the water replaced with filtered (0.2 µm) and UV-treated fresh artificial seawater (Instant Ocean) three times weekly. At the same time, cultures were fed *Rhodomonas salina* (UTEX LB 2763) at a density of 2000 cells/mL and

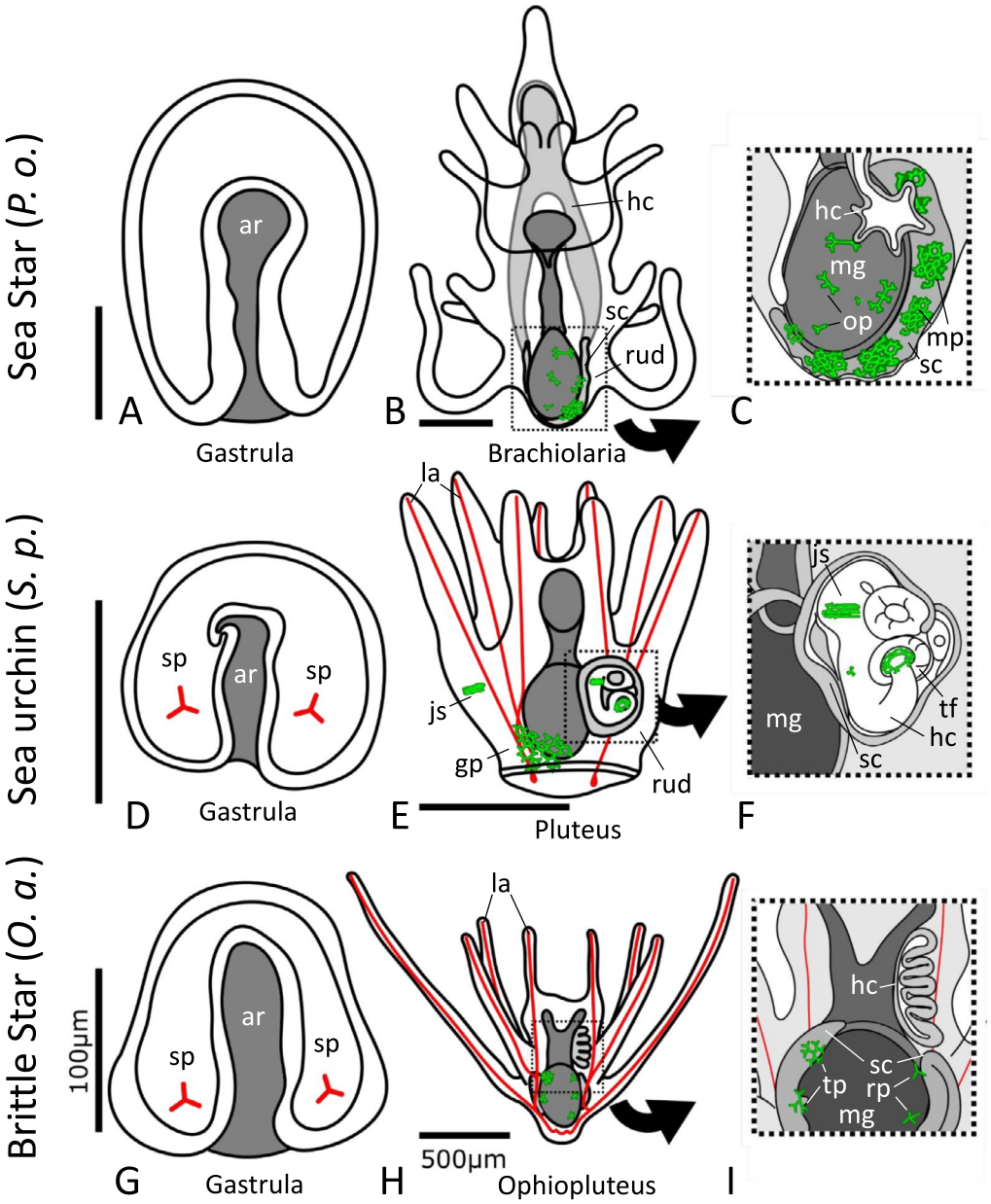

Fig. 2 Larval and juvenile skeletogenesis in sea star, sea urchin, and brittle star larvae. Larval skeleton is depicted in red, while juvenile skeleton is depicted in green. **A** Sea star gastrula (*Pisaster ochraceus*). No skeleton is present. **B** Sea star brachiolaria (*P. o.*). Adult skeleton develops in the somatocoel/rudiment. **C** Close-up of sea star rudiment (*P. o.*) skeletogenesis begins with small spicules, developing into the plates of the juvenile test. **D** Sea urchin gastrula (*Strongylocentrotus purpuratus*). Skeletogenesis begins with spicules at the ventrolateral clusters. These spicules will elongate and form the post-oral and anterolateral larval arms. **E** Sea urchin pluteus larva (*S. p.*). Juvenile skeletogenesis typically begins with the genital plate adjacent to the gut and tube feet/juvenile spines in the rudiment. **F** Close-up of sea urchin rudiment (*S. p.*) Tube feet and spines in the rudiment are among the first skeletal structures formed. **G** Brittle star gastrula (*Ophiopholis aculeata*) Skeletogenesis begins with spicules at the ventrolateral clusters. These spicules will elongate and form the post-oral and anterolateral larval arms. **H** Brittle star ophiopluteus (*O. a.*) Adult skeletogenesis begins adjacent to the gut with the formation of terminal and radial plates. **I** Close-up of ophiopluteus (*O. a.*) gut and hydrocoel. ar: archenteron, hc: hydrocoel, sc: somatocoel, rud: rudiment, mg: midgut, op: oral plate, mp: madreporitic plate, la: larval arm, js: juvenile spine, gp: genital plate, tf: tube foot, tp: terminal plate, rp: radial plate

Dunaliella tertiolecta (UTEX LB 999) at 3000 cells/mL. Gastrulae were collected for skeletogenesis assays at 2–3 dpf. Late pluteus larvae were collected for skeletogenesis assays at 27 dpf.

We collected Adult *Pisaster ochraceus* by hand during low tide at Friday Harbor, Washington (2019) and maintained them in seawater tables under flow-through seawater conditions [45]. After spawning and fertilization, hatched embryos were transferred to 2 L jars at a density of 1 larva per 2 mL. The cultures were cleaned manually and had the water replaced with fresh seawater three times weekly. At the same time, cultures were fed *Rhodomonas* sp. at a density of 3000 cells/mL and *Dunaliella* sp. at 4000 cells/mL. Gastrulae were collected after 48 h at 11–13 °C and staged to ensure they were at early gastrulation (after ingression of primary mesenchyme cells and invagination of the blastopore, but before ingression of secondary mesenchyme cells and archenteron contact with the animal pole; see [71] for review of gastrulation). Early bipinnaria were collected after 12 dpf, after coelomic pouch elongation. Late bipinnaria were collected at 22 dpf, just before formation of the brachiolaria arm buds.

Adult urchins (*Strongylocentrotus purpuratus*) were shipped from Monterey, CA (2019–2023), where they were collected by diving and subsequently kept in tanks of artificial seawater at the Hagen Aqualab (University of Guelph, ON). The adults were fed a diet of kelp (*Macrocystis pyrifera*, and *Kombu spp.*) every 2–3 days. Temperature was maintained at 14°C and salinity at 31 ppt). Urchins were spawned by injecting 0.5–1.5 mL of 0.5 M KCl in distilled water, depending on the size of the urchin. Sperm was collected dry by pipetting sperm directly from the gonopores. Females were inverted over a beaker of filtered artificial seawater (0.2 µm—FASW) to collect eggs. After spawning, eggs were washed twice with FASW. Diluted sperm (approx. 1:100) was titrated into the beaker of eggs until fertilization success reached at least 90%. Fertilized eggs were washed once more with FASW to remove excess sperm and allowed to develop at 12 °C in a 2 L beaker until hatching. After 48 h at 12–14 °C, hatched embryos were transferred to 2 L beakers at a density of 1 larva/mL. Sea urchin larval cultures were maintained at 14 °C with salinity at 31–33 g/L and larval density was gradually reduced on a weekly basis to an eventual density of approximately 250 larvae per liter. Cultures were stirred constantly using a paddle system previously described by Strathmann [100] and kept on a 12:12 light cycle. The cultures were cleaned manually and had the water replaced three times weekly. At the same time, cultures were fed *Rhodomonas salina* at a density of 3000 cells/mL and *Dunaliella tertiolecta* at 4000 cells/mL.

Dendraster excentricus (sand dollars) were collected from Crescent Beach, East Sound, Orcas Island (WA, USA) in 2019. *D. excentricus* were spawned by injecting 0.2–1.0 mL of 0.5 M KCl in distilled water, depending on the size of the animal. Sperm was collected dry by pipetting sperm directly from the gonopores. Females were inverted over a beaker of natural seawater to collect eggs. After spawning, eggs collected by pipette and distributed in a monolayer in a 500 mL beaker of seawater. Diluted sperm (approx. 1:100) was titrated into the beaker of eggs until fertilization success reached at least 90%. Fertilized eggs were washed once with seawater to remove excess sperm and allowed to develop at 11–13 °C in a 500 mL beaker until hatching. After 20 h at 14 °C, hatched embryos were transferred to 2 L jars at a density of 1 larva/mL. Gastrulae were collected shortly thereafter and staged to ensure they were at early gastrulation.

Hormone preparation

Thyroid hormones (rT3, T4, T3) were prepared as described in Ref. [104] (dissolved in filtered artificial seawater with 1% DMSO at a working concentration of 10^{-3} M). PD98059 (inhibitor of MAPK ERK1/2 phosphorylation by MEK1, Sigma-Aldrich P215) and RGD peptide (inhibitor of integrin RGD-binding pocket; Sigma-Aldrich A8052) were also used, and similarly diluted in filtered artificial seawater to a working concentration of 10^{-3} M. Hormones and inhibitors were diluted from the working stock, and larvae were exposed to a final concentration of 10^{-7} M rT3, T4, T3, or RGD peptide, or to 5×10^{-5} M PD98059. Although UO126 has been previously used to inhibit MEK in sea urchins (e.g., [34]), we used PD98059 because it has previously been used to inhibit the TH-integrin signaling pathway (e.g., [52, 104]). U0126 is an inhibitor of MEK1/2, while PD98059 selectively inhibits MEK1. As PD98059 was successful in inhibiting TH acceleration of skeletogenesis, it is likely the optimal choice as PD98059 would avoid some additional effects on MEK2, which may be less involved in the integrin signaling pathway. Concentrations were chosen based on optimal concentrations in Taylor and Heyland [104].

Skeletogenesis assays

Skeletogenic assays were conducted as described in Taylor and Heyland [102, 104]. We scored the presence of skeletal spicules in repeated measures of individually isolated live larvae and determined the proportion of individuals which had developed skeleton (hourly for gastrulae, daily for late-stage larvae). Presence of skeletal spicules was confirmed with polarized light microscopy. Experiments were considered complete when at least one group asymptotically reached skeletogenesis (over 95%

of at least one group achieved skeletogenesis), typically over the course of 4 h for gastrulae, or 3–5 days for late-stage larvae (*S.p.* gast.: 4 h, *S.p.* larvae:, *P.o.* gast.: 72 h, *P.o.* larvae: 120 h, *D.e.* gast.: 4 h, *O.a.*: gast: 5 h, *O.a.* larvae: 96 h). Schematic of methodology can be found in Figure S5 (BC). Larvae were kept at a density of 1 larva/mL in individual wells (24 well plate, 1 mL/well). Larvae were placed on a slide for observation and skeletal structures were detected by polarized light microscopy on a compound microscope with inserted polarizing filter. Echinoderm skeletons are composed of a single birefringent crystal and polarized light microscopy is extremely suitable for detection of even initial skeletal spicules. In the case of gastrulae, skeleton was detected and scored at the ventrolateral clusters. In the case of late-stage larvae, the presence of adult skeleton developing in and around the rudiment was scored. Any skeleton which was not part of the larval arms was considered to be adult skeleton [41].

Fluorescent microscopy

Fluorescently labeled thyroxine (RHT4) was synthesized as described in Taylor and Heyland [104] and used to determine T4-binding locations. RHT4 is a fluorescently labeled TH analog which has been validated as binding to TH receptors (e.g., [13, 14, 102]). RHT4 was prepared at a stock concentration of 10^{-3} M and diluted in PBS to a final concentration of 10^{-6} M for staining fixed samples. M8159 (antibody for phosphorylated ERK1/2; mouse monoclonal, Sigma-Aldrich M8159; e.g., [88]) was used to quantify MAPK (ERK1/2) phosphorylation (1:250). Hoechst 33342 (working stock 1 mg/mL, final concentration 5 µg/mL) was used to stain and identify nuclei. Thyroid hormones were diluted in filtered artificial seawater with DMSO (5:95 DMSO: FASW) to a working stock concentration of 10^{-3} M before being diluted to a final concentration of 10^{-7} M in exposure conditions.

Larvae or gastrulae were exposed to 100 nM T4, 500 µM PD98059, 100 nM RGD peptide, 100 nM rT3, 100 nM RGD + 100 nM T4 or a vehicle control (FASW with 0.0005% DMSO) for 90 min. Subsequently, they were fixed in 2% formaldehyde for 10 min at room temperature and washed with methanol and placed for 5 min in a − 20 °C freezer. Samples were washed 3 × with phosphate-buffered saline with 0.1% Tween-20 (PBST; 5 min between washes) at room temperature and blocked with 1% Goat Serum in PBST for 60 min. Samples were exposed to primary MAPK antibody (M8159 1:250) for 12 h overnight at 4 °C. They were then washed 5 × in PBST (5 min between washes) and exposed to secondary antibody for 4 h (1:1000). This was followed by 7 × washes in PBS (5 min between washes). Finally, samples were exposed to a mixture of Hoechst 33342 (5 µg/mL) and RHT4 (10^{-6} M) in PBS for 15 min, followed by 3 × washes in PBS and were then mounted for imaging in DABCO/glycerol (see similar protocol in [113]). As the previously reported magnitude of TH effects on MAPK phosphorylation was over threefold increase in intensity [104], a sample size of 4–6 confocal images was predicted to be sufficient statistical power to test the effect of T4 on MAPK phosphorylation. Schematic of methodology can be found in Figure S5 (A).

For identifying thyroxine in sea urchin gastrulae, we used a monoclonal antibody against thyroxine (Fisher Scientific, ab30833), using immunohistochemistry (IHC) following procedures previously described in mouse embryos. Embryonic stages (41 h and 48.5 hpf) were fixed in 4% paraformaldehyde in artificial seawater (red sea salt) for 12 min at room temperature and washed three times in 1 × PBS (ph: 7). Embryos were then processed in PBST (1 × PBS with Triton-X100 at 0.3%) through three washes at 5 min each and then added to blocking agent (1% goat serum in 1xPBST). Primary antibody was prepared at a final concentration of 1:800 in blocking agent and embryos were incubated overnight at 4C. Negative controls were prepared using thyroxine (SIGMA) in DMSO at 10^{-2} M concentration and mixed 1:1 with monoclonal antibody, incubated at room temperature for 72 h. After five washes in block solution, embryos were exposed to secondary antibody (Alex-Fluor, mouse-anti goat, Fisher Scientific, A-11005) at 1:800 dilution overnight at 4 C. After 5 brief washes in PBS, embryos were mounted in DABCO (SIGMA D27802) with Hoechst (1:800) on slides and imaged. Imaging was conducted on a Nikon Ti2 inverted microscope. Images were processed using deconvolution software NIS-Elements (3D automatic; Wide-field Modalit; NA: 1.2; RI: 1.330. Z projections and dynamic contrast was adjusted using NIS elements.

Statistical analysis

MAPK phosphorylation was quantified by automatic cell counting in the Hoechst 33342 channel, followed by a measurement of fluorescent intensity of each individual cell in a radius around each nucleus (see S1 for details and S5 for ImageJ script). Intensity was normalized to the Hoechst 33342 signal to account for attenuation (Figure S1). Fluorescent intensity of the top 5% of cells was compared between experimental groups and the control by one-way ANOVA followed by Tukey's post hoc test. In addition, primary mesenchyme cells and secondary mesenchyme cells were identified in sea urchin gastrulae, and fluorescence quantified, normalized to Hoechst 33342 signal intensity. PMCs and SMCs were identified primarily by their location and morphology, each being distinctive and identifiable (mesenchymal cells arranged in a syncytial ring at the vegetal pole, or clusters

of mesenchyme cells at the animal pole respectively). In brittle star ophioplutei, we identified and quantified fluorescence intensity in the ciliated band, hydrocoel, midgut, posterior coelom/somatocoel, and presumptive skeletogenic mesenchyme cells along the skeletal rods. Intensities and means are reported as ± standard error. Colocalization of Hoechst nuclear stain, MAPK phosphorylation, and T4-binding locations in juvenile rudiments and midgut in late-stage larvae was measured with Pearson's Coefficient using JACoP (v2.0; [6]).

For the skeletogenic assays, experimental groups were compared with binary logistic regression of skeletal presence (binomial) and time (hours or days) contrasted to the control group. In addition, spicule proportion over time was transformed to a rate of skeletogenesis (spicules/hour or spicules/day) and compared to the control with one-way ANOVA followed by Tukey's post hoc. Proportions and means are reported as ± standard error.

Results

Thyroid hormone effects on skeletogenesis

Thyroid hormone exposure (T4, T3) accelerated initiation of skeletogenesis in a sea urchin (*Strongylocentrotus purpuratus*), a brittle star (*Ophiopholis aculeata*), and a sea star (*Pisaster Ochraceus*) (Fig. 3), as well as a sand dollar (*Dendraster excentricus*; Figure S1 and as previously shown in Ref. [41]). However, we did not observe induction of skeletogenesis in TH-exposed groups of *Pisaster ochraceus* (sea star) gastrulae ($n=20$, ANOVA not possible as no groups produced skeleton; $p=1.00$). TH exposure, including T4 and T3, accelerated onset of juvenile skeletogenesis ($n=6$, F (7,40) = 36.25, $p<0.001$) in sea star bipinnaria. Sea star bipinnaria exposed to both THs and PD9809 or RGD peptide displayed a lower level of skeletogenesis than groups exposed to THs alone (Tukey's HSD, $p<0.001$).

THs, including T4 and T3, accelerated initiation of skeletogenesis in *O. aculeata* gastrulae ($n=20$, F (7152) = 12.45; $p<0.001$; Tukey's HSD, T4: 95% CI [1.75-fold, 2.69-fold], T3: 95% CI [1.08-fold, 2.03-fold]). Groups exposed to both THs and an inhibitor (RGD peptide (RGD) or PD98059 (PD)) displayed a lower level of skeletogenesis than groups exposed to THs alone (Tukey's HSD, $p<0.001$). In *O. aculeata* larvae, THs (T4) accelerated juvenile skeletogenesis ($n=12$, F (3,44) = 24.22; Tukey's HSD $p<0.001$). The rate of skeletogenesis was lower in T4 + PD98059 than in T4-exposed groups ($p=0.0163$). The effect of RGD peptide on skeletogenesis was not tested in late-stage *O. aculeata*.

In all cases, T4 at 10^{-7} M had a stronger effect on initiation of skeletogenesis than T3 at 10^{-7} M (1.22-fold [*S.p.* 8-armed pluteus] to 3.71-fold [*S.p.* gastrula], $\bar{x}=2.31$-fold). This difference was statistically significant in all cases except late-stage *S. purpuratus* (8-armed pluteus stage; Tukey's HSD, alpha = 0.05). Gastrulae exposed to T4 showed rapid skeletogenesis (< 5 h; Fig. 3M) in the ventrolateral clusters (Fig. 3A, B, E, F) in sea urchin and brittle stars, but not sea stars (Fig. 3 I, J). This acceleration of skeletogenesis occurred over the course of 5 h observation, shifting the onset of skeletogenesis forward by 1.05 h (± 0.07 h) in *S. purpuratus* (sea urchin) gastrulae and 1.12 h (± 0.13 h) in *O. aculeata* gastrulae. This represents a significant increase in the rate of skeletogenesis in T4-exposed gastrulae (*S. purpuratus*: 3.13-fold, ± 0.26; *O. aculeata*: 2.22-fold, ± 0.31).

THs accelerated skeletogenesis in older larvae of all three classes of Echinoderms (sea urchin, sea star, and brittle star; Fig. 3N). Sea urchin larvae displayed increased skeletogenesis in the developing rudiment, as well as extra-rudiment skeleton such as juvenile spines and genital plates. Over the course of 7 days of observation, T4-exposed larvae developed skeleton in the juvenile rudiment 2.78 days in advance of the control group (1.70-fold increased rate, ± 0.14) and had an average rudiment skeletal development stage of 8.4 compared to the control group at 0.7 (staging scheme from [41]).

(See figure on next page.)

Fig. 3 Thyroid hormones accelerate initiation of skeletogenesis in sea urchins, sea stars, and brittle stars. Arrowheads (▶) indicate skeletogenesis. **A** Sea urchin gastrula in control conditions. **B** Sea urchin gastrula after T4 exposure for 20 h at 10^{-7} M. Skeletogenesis is taking place in the ventrolateral clusters. **C** Sea urchin pluteus gut and rudiment. Skeletogenesis is visible in the genital plate and as a small single spicule in the rudiment. **D** Sea urchin pluteus gut and rudiment after T4 exposure for 5 days at 10^{-7} M. Skeletogenesis is dramatically accelerated with multiple skeletal plates, juvenile spines, and tube-foot rings observed. **E** Ophiuroid gastrula at the beginning of skeletogenesis. **F** Ophiuroid gastrula after T4 exposure for 24 h at 10^{-7} M. Skeletogenesis has been accelerated and the larval arms have begun to form. **G** Ophiuroid ophiopluteus gut region. Somatocoel has not yet begun to form skeleton. **H** Ophiuroid ophiopluteus gut region after T4 exposure for 48 h at 10^{-7} M. Several skeleton spicules are visible. **I** Sea star early bipinnaria. No skeletogenesis is present. **J** Sea star early bipinnaria after T4 exposure during gastrulation for 3 days at 10^{-7} M. No skeletogenesis is present. **K** Sea star late bipinnaria gut. No skeletogenesis is present. **L** Sea star late bipinnaria gut after T4 exposure for 24 h at 10^{-7} M. T4 dramatically accelerates skeletogenesis adjacent to the gut. **M** Quantification of skeletogenesis (mean spicule presence per hour) during gastrulation reveals that thyroxine (T4) accelerates skeletogenesis in sea urchin ($n=20$) and ophiuroid gastrulae ($n=24$), but not sea star larvae ($n=20$; t-test, $p<0.05$). Asterisk indicates significant difference from the control. **N** Quantification of juvenile skeletogenesis (mean spicule presence per day) reveals that thyroxine (T4) accelerates skeletogenesis in sea urchin ($n=12$), ophiuroid ($n=12$), and sea star late-stage larvae ($n=30$; t-test, $p<0.05$). Asterisk indicates significant difference from the control

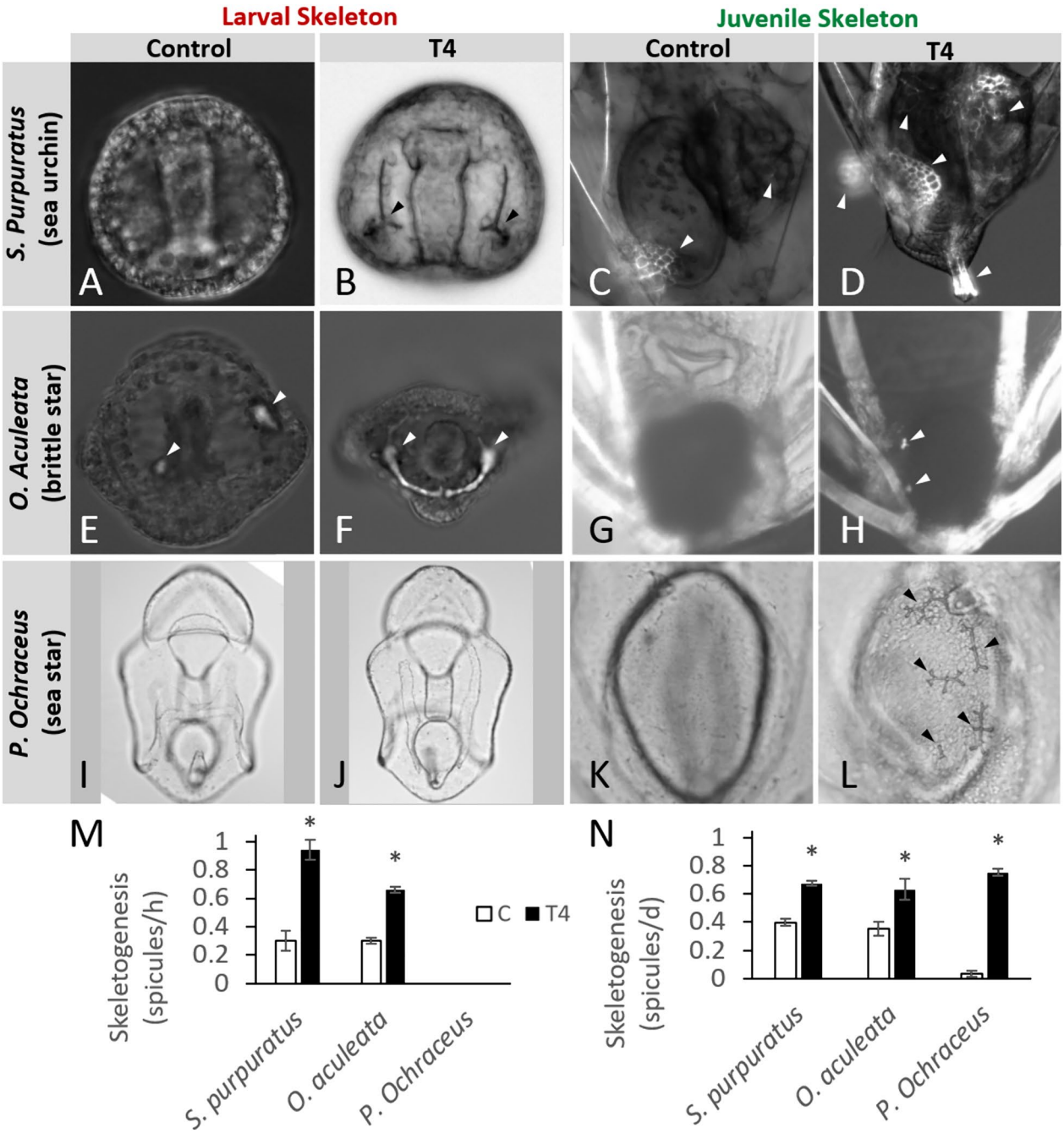

Fig. 3 (See legend on previous page.)

T4 accelerated juvenile skeletogenesis of brittle star ophioplutei (23 d) in the terminal and radial plates adjacent to the gut and somatocoel (Fig. 3H). T4 brought forward the mean initiation of juvenile skeletogenesis by 0.96 d, resulting in a 1.79-fold (±0.29) increase in the rate of skeletogenesis relative to the control. At the end of observation (27 days, 4 days post-exposure), every larva had begun juvenile skeletogenesis.

T4 drastically accelerated skeletogenesis of sea star late bipinnaria/early brachiolaria larvae (24 days). After 24 h of T4 exposure, *P. ochraceus* bipinnaria larvae produced skeletal spicules (oral plates) adjacent to the gut and somatocoel (Fig. 3L). By day 3, every single T4-exposed larva had produced skeleton, including oral and madreporitic plates, while not a single control larva had begun skeletogenesis (Fig. 3K). At the end of

observation (29 days, 5 days post-exposure), 5/30 (± 2.7) of control larvae had produced skeleton. This represents a 4-day acceleration of skeletogenesis by T4, and a 22.6-fold (± 5.7) increase in the rate of skeletogenesis over the observed period.

Thyroid hormone signaling mechanisms

D. excentricus gastrulae exposed to both RGD peptide (a competitive inhibitor of the RGD-binding pocket on RGD-binding integrins) and T4 showed less acceleration of larval skeletogenesis relative to the control than larvae exposed to T4 alone (Figure S4). This effect was also observed in *S. purpuratus* (Fig. 4A), and *O. aculeata* gastrulae (Fig. 4C), as well as during juvenile skeletogenesis in *P. ochraceus* late bipinnaria (Fig. 4E; binomial logistic regression, $n = 12–40$, $p < 0.05$). Groups exposed to PD98059, an inhibitor of MAPK phosphorylation (ERK1/2), as well as T4, showed a decrease in acceleration of initiation of skeletogenesis relative to the control. This effect was observed in *S. purpuratus* and *O. aculeata* gastrulae (Fig. 4AC), as well as during juvenile skeletogenesis in *P. ochraceus*, *S. purpuratus*, and *O. aculeata* late-stage larvae (binomial logistic regression, $n = 12–40$, $p < 0.05$). However, PD98059 had little to no effect alone (Fig. 4D–F). *P. ochraceus* gastrulae did not produce skeleton either with or without thyroid hormone exposure and as such there were no differences in rate of skeletogenesis between any *P. ochraceus* gastrulae treatment groups (Fig. 4B).

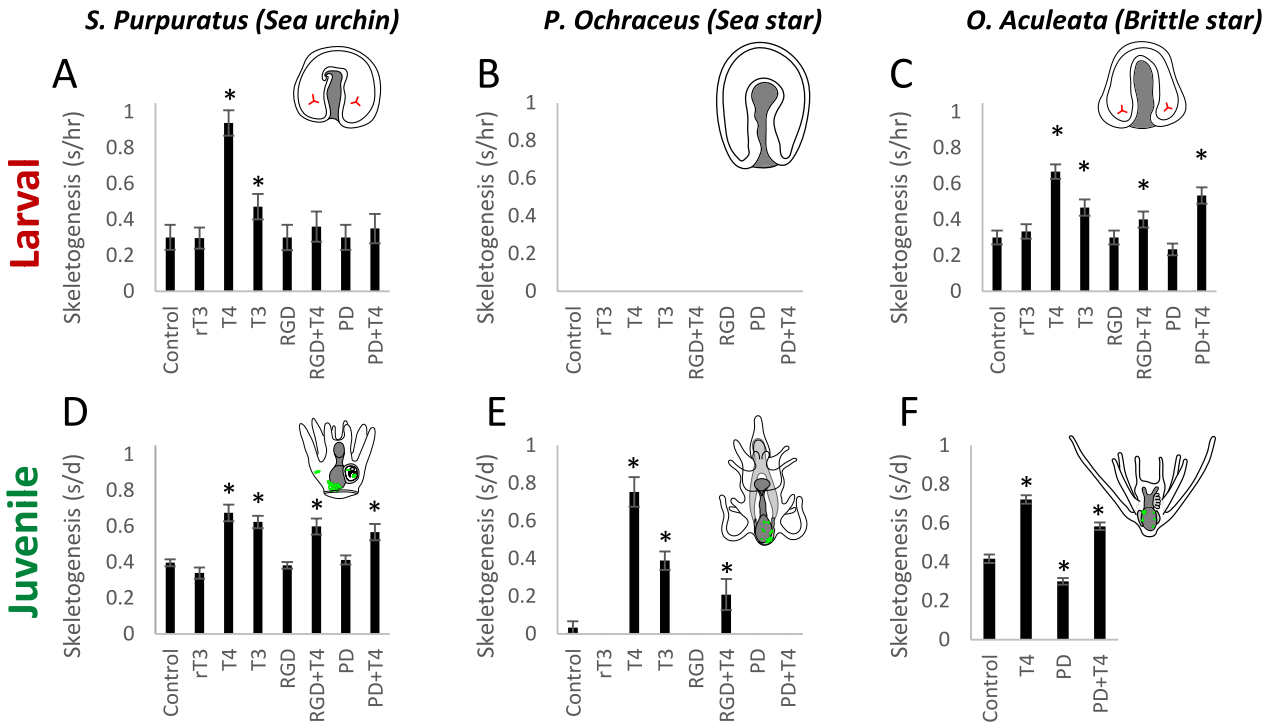

Fig. 4 Inhibitors of MAPK phosphorylation and integrin binding inhibit the effect of thyroid hormones on skeletogenesis in sea urchin, brittle star, and sea star gastrulae and larvae. Larvae were exposed to the thyroid hormones, rT3, T3, and T4 (10^{-7} M), RGD peptide (RGD; 10^{-7} M) or PD98059 (PD; 5×10^{-7} M). **A** Sea urchin gastrulae. Thyroid hormones, including T4 and T3, accelerate initiation of skeletogenesis in sea urchin gastrulae relative to the control ($n = 20$, F (7152) = 9.20; Tukey's HSD, $p < 0.00001$, T4: 95% CI [2.06-fold, 4.16-fold], T3: 95% CI [1.57-fold, 2.62-fold]). RGD peptide and PD98059 inhibit the effects of T4 on skeletogenesis (Tukey's HSD, $p < 0.00001$). Data reproduced from [106]. **B** Sea star gastrulae. THs were not found to induce skeletogenesis in sea star gastrulae ($n = 20$, ANOVA not possible, all groups identical; $p = 1.00$). Sea star gastrulae do not contain the cell type necessary for skeletogenesis. **C** Brittle star gastrulae. Thyroid hormones, including T4 and T3, accelerate initiation of skeletogenesis in Brittle star gastrulae ($n = 20$, F (7152) = 12.45; $p < 0.00001$; Tukey's HSD, T4: 95% CI [1.75-fold, 2.69-fold], T3: 95% CI [1.08-fold, 2.03-fold]). RGD peptide (RGD) and PD98059 (PD) partially inhibit the effects of THs on skeletogenesis (Tukey's HSD, $p < 0.0001$). **D** Sea urchin pluteus larva. Thyroid hormones accelerate juvenile skeletogenesis ($n = 12$, F (10,121) = 20.88, $p < 0.00001$), even in the presence of RGD peptide, or PD98059 ($p = 0.0023$, 0.019). A higher dosage of RGD peptide/PD98059 was previously found to inhibit skeletogenesis (Taylor 2021). Data reproduced from [106]. **E** Sea star bipinnaria larva. Thyroid hormones accelerate, including T4 and T3, juvenile skeletogenesis ($n = 6$, F (7,40) = 36.25, $p < 0.00001$). The effect of thyroid hormones is inhibited by PD9809 and RGD peptide (Tukey's HSD, $p < 0.00001$). **F** Ophiopluteus larva. Thyroid hormones (T4) accelerate juvenile skeletogenesis ($n = 12$, F (3,44) = 24.22; Tukey's HSD $p < 0.00001$). This effect is partially inhibited by PD98059 ($p = 0.0163$). The effect of RGD peptide on skeletogenesis was not tested in late-stage *O. aculeata*. Asterisk indicates significant difference from the control

T4-binding locations and colocalization with induced MAPK phosphorylation

Thyroid hormone exposure increased MAPK phosphorylation in *S. purpuratus* gastrulae ($n=4$, $p<0.05$). RGD peptide alone had no statistically significant effect on MAPK phosphorylation, but did inhibit the effect of T4 ($n=4$, $p<0.05$). THs (T4) bound to PMCs in sea urchin gastrulae (Fig. 5B), as well as to regions near the tip of the developing archenteron. MAPK activation was seen most strongly in secondary mesenchyme cells (neural precursors) and the coelomic pouches (rudiment precursors), as well as to a lesser degree in PMCs ingressing at the vegetal pole. However, MAPK phosphorylation induced by T4 exposure was primarily located in the PMCs ($p<0.01$). Both MAPK activation and T4-binding locations appeared to be localized mainly to the cytoplasm (Fig. 5) with limited binding to the nucleus/membrane, contrasting with previously published results showing primarily membrane binding. Typically, the site of MAPK phosphorylation was colocalized with T4-binding sites within the cell (Fig. 5C′′–C‴, D′′–D‴) in the PMCs, and to a lesser degree, the SMCs, but not in the coelomic pouches.

T4 did not significantly increase MAPK phosphorylation in *P. ochraceus* gastrulae ($t[8]=0.526$, $p=0.61$; Fig. 6E). RGD peptide decreased MAPK phosphorylation ($t[8]=2.80$, $p=0.023$; Fig. 6E). No distinct T4-binding sites were detected in either the control (Fig. 6A, C) or T4-exposed larvae (Fig. 6B, D). MAPK phosphorylation was most active in the developing coelomic pouches and was asymmetrical in all samples (20/20).

T4 bound primarily to the midgut, hindgut, and somatocoel in sea star bipinnaria (Fig. 7) and brachiolaria (Fig. 8). T4-exposed larvae displayed higher levels of MAPK phosphorylation in both bipinnaria and brachiolaria ($t(10)=3.42$, $p=0.007$; Fig. 8B; *P. ochraceus*). In contrast, RGD peptide exposure resulted in a decrease in MAPK phosphorylation as well as inducing whole-body muscle contractions (Figure S2). Larvae exposed to both RGD peptide and T4 displayed no statistically significant difference in MAPK phosphorylation from the control group ($t(10)=1.31$, $p=0.218$).

In bipinnaria, the region of strongest MAPK phosphorylation was the somatocoel (Fig. 7). T4 bound most strongly to the membrane of gut cells, predominantly at the cell–cell junctions, but also to the nucleus (Fig. 7C′′). MAPK phosphorylation in the gut was strongly colocalized to cells which bind T4 (Fig. 7C′′'). Few presumptive T4-binding sites were observed in the hydrocoel, although the adjacent midgut did bind T4 (Fig. 7B).

We observed increased T4-binding sites in older sea star brachiolaria (Fig. 8). Putative T4-binding cells in the hindgut adjacent to the extending somatocoel were numerous and intensely fluorescent. Unlike in the bipinnaria, we observed T4-binding sites in the hydrocoel. As well, T4-binding sites were occasionally observed in the membrane/cytoplasm but frequently colocalized well with nuclear stains (Fig. 8D, E; $\bar{r}(4)=0.715$). Some MAPK phosphorylation was observed, which corresponded to T4-binding locations, primarily in the midgut and hindgut (Fig. 8C, E), but not the hydrocoel (Fig. 8D).

In late-stage ophiuroid larvae (eight-armed ophiopluteus), T4 bound to the gut, somatocoel, and presumptive skeletogenic mesenchyme in posterolateral arms (Fig. 9A, B, F). In the posterolateral arms, we detected T4-binding sites predominantly in mesenchymal cells adhering to the skeletal rod (Fig. 9C, F). Most skeleton-adhering T4-binding cells displayed increased MAPK phosphorylation in response to T4 exposure. T4 significantly increased MAPK phosphorylation in presumptive skeletogenic cells in the posterolateral arms of *O. aculeata* ophioplutei ($t(6)=2.594$, $p=0.041$; Fig. 9G). T4 did not increase phosphorylation in the hydrocoel (Fig. 9D) or ciliated band. As well, we detected a trend towards increased MAPK phosphorylation in the somatocoel/posterior coelom which was not statistically significant (Fig. 9E, G, $p>0.05$). The effect of T4 on total MAPK phosphorylation is potentially inhibited by RGD peptide with a mean decrease of 17% MAPK phosphorylation fluorescent intensity, although this difference was not statistically significant ($t(6)=1.08$, $p=0.320$).

We imaged larvae with a variety of hydrocoel developmental stages, from the beginning of metamorphic development until the point at which the hydrocoel begins to wrap around the gut. A representative T4-exposed larva at the relatively advanced 5-lobed stage is depicted in Fig. 9B, E. No larvae examined displayed a high degree of T4-binding in the hydrocoel. In contrast, the somatocoel of most larvae presented with presumptive T4-binding sites, and T4-exposed samples showed a greater intensity of MAPK phosphorylation in the somatocoel, colocalized with T4-binding sites (Fig. 9F; $\bar{r}(6)=0.748$).

In sea urchin (*S. purpuratus*) eight-armed pluteus larvae (rudiment soft tissue stages v–vii; [41]), RHT4 bound and fluoresced to gut cells, indicating potential T4-binding sites (as in the other echinoderms we examined). In addition, T4 bound to the rudiment, primarily to the rapidly developing layer most distal to the gut. In T4-exposed larvae, MAPK phosphorylation was induced in the gut and rudiment, strongly colocalized with putative T4-binding sites ($\bar{r}(6)=0.862$). A close examination of binding sites in the T4-exposed larvae showed T4 binding in both the nucleus and cell membrane (Fig. 10B). Nuclear binding was primarily observed in the rudiment ($\bar{r}(6)=0.847$), compared to the gut ($\bar{r}(6)=0.459$). This is in contrast with *S. purpuratus* gastrulae and control

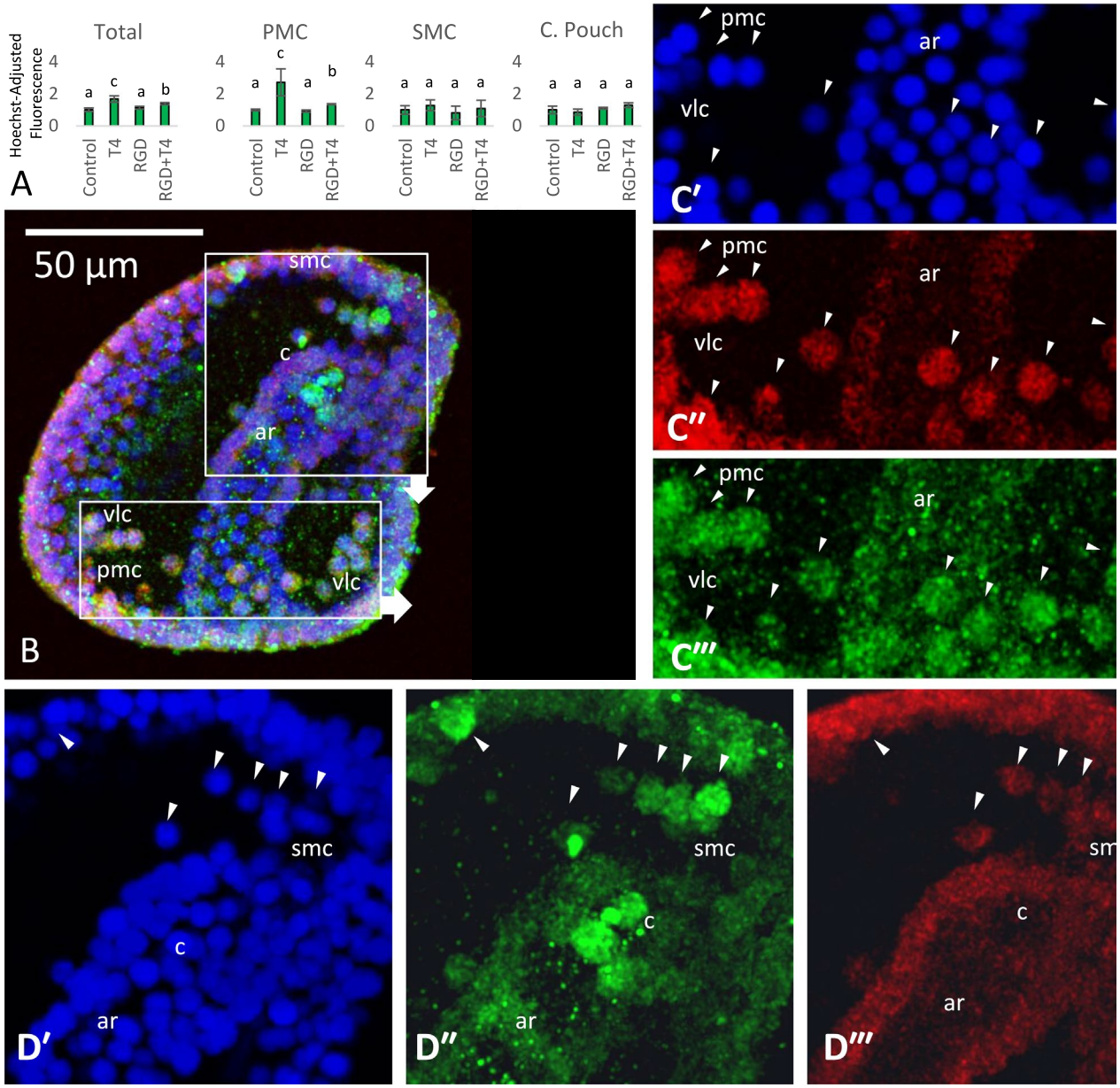

Fig. 5 Putative MAPK-P and T4-binding site distribution in *Strongylocentrotus purpuratus* gastrulae. Gastrulae were exposed for 90 min prior to fixation. Gastrulae were stained with Hoechst 33342 (blue; nuclei), rhodamine-conjugated T4 (red; T4-binding sites), and an antibody for phosphorylated MAPK (green, P-MAPK). Fluorescent debris exterior to gastrula was removed. **A** T4 increases MAPK intensity in S. p. larvae ($n = 4$, $p < 0.05$; significant differences exist between cell types with no shared letter). This effect may be partially inhibited by RGD peptide ($p < 0.05$). The increase in MAPK phosphorylation is present in PMCs, but not SMCs or the coelomic pouch ($n = 4$, $p < 0.05$). Both SMCs and the coelomic pouch presented with a high degree of MAPK phosphorylation in both the T4-exposed and control groups. **B** Maximum intensity projection of confocal fluorescent image of *S. p.* gastrula. **C–C‴** Focal slice of gastrula showing primary mesenchyme cells (PMCs) and lower archenteron. Arrowheads (▶) PMCs. PMCs display greater T4 binding and MAPK phosphorylation than surrounding cells. Ventrolateral clusters have formed (vlc). **D–D‴** Focal slice of gastrula showing tip of the archenteron and developing coelomic pouches, as well as secondary mesenchyme cells (SMCs). Arrowheads (▶) identify SMCs. SMCs and the coelomic pouches display greater MAPK phosphorylation than surrounding cells. T4 binding is slightly elevated in regions near the tip of the archenteron and small protein clusters in SMCs. c: Coelomic pouch, ar: Archenteron (gut), pmc: primary mesenchyme cells, smc: secondary mesenchyme cells, vlc: ventrolateral cluster

late-stage plutei which both showed binding primarily in the cytoplasm with potential membrane/nuclear binding (Fig. 5B–D).

We found that sea star gut displayed highly asymmetrical putative T4-binding locations, with increased quantity and intensity of binding sites in the midgut and foregut closer to the somatocoel (Fig. 11). We observed possible T4-binding sites predominantly in the basal cell membrane of gut epithelia, as well as the membrane of gut-adjacent mesenchyme cells. Many of these cells also display binding in the nucleus, albeit to a lesser degree ($\bar{r} = 0.566$). There are more T4-binding cells adjacent to the somatocoel and the intensity of T4-binding appears to be higher adjacent to the somatocoel. In T4-exposed larvae, these locations colocalize approximately with increased MAPK phosphorylation in the gut, and to a lesser degree, the somatocoel and mesenchyme cells adhering to the gut/somatocoel boundary ($t(10) = 3.594$, $p = 0.0049$; Fig. 10B) relative to control larvae (Fig. 11A). RGD peptide prevents the effect of T4 on MAPK phosphorylation ($t(10) = 3.16$, $p = 0.010$), but potentially increases the number of T4-binding locations we observed ($p = 0.023$; Fig. 11C).

T4 presence in sea urchin gastrulae

We identified a cluster of cells at the tip of the developing archenteron containing thyroxine, based on IHC (Fig. 12). Negative controls did not show any specific staining in that area. The cells are thyroxine positive before embryonic skeleton formation and are present until gastrulation is completed and the mouth is formed.

Discussion

We found that THs (T4 and T3) accelerated skeletogenesis in larvae of distantly related echinoderm groups (sea stars, brittle stars, and sea urchins), suggesting a conserved regulatory mechanism of skeletogenic mesenchyme by THs. T4 bound to cells near sites of skeletogenic activity and increased MAPK phosphorylation. Both the acceleration of skeletogenesis and the MAPK phosphorylation was inhibited by RGD peptide (a competitive inhibitor of RGD-binding integrins), as well as PD98059 (an inhibitor of MAPK [ERK1/2] phosphorylation) in all species. These results provide further evidence for a role of non-genomic TH signaling (signaling which does not proceed via the canonical nuclear hormone receptor mechanism) via an integrin membrane receptor-mediated MAPK cascade and suggests a conserved regulatory mechanism between these groups. However, PD98059 had no significant on skeletogenesis alone, with the exception of O. aculeata larvae, suggesting that either the concentration of PD98059 was insufficient, that PD98059 failed to sufficiently inhibit MAPK phosphorylation, or that MAPK signaling may be less important for skeletogenesis than expected.

On a subcellular level, THs bind to the cytoplasm, membrane, and nucleus in echinoderms. We found nuclear binding to be more prominent in older echinoderm larvae, especially in *P. ochraceus* brachiolaria midgut and *S. purpuratus* rudiment nuclei, as well as in *D. excentricus* gastrulae. This coincides with evidence suggesting genomic transcriptional regulation is much more prominent in sea urchin eight-armed plutei relative to gastrulae [106] and reports that TH levels rise in older larvae as they develop to metamorphosis [15]. THs accelerate sea urchin rudiment development [15, 44, 104], suggesting that the rudiment may be a primary site of genomic TH signaling and regulation of metamorphosis.

We found that sea star bipinnaria showed the greatest acceleration of skeletogenesis by thyroid hormones in the late-larval stages, with THs inducing skeletogenesis weeks in advance of typical development (e.g., [83]). This might be attributed to the early presence of coelomic mesenchyme adjacent to the gut, relative to *S. purpuratus* and *O. aculeata*, where late mesenchymal cells responsible for skeletogenesis do not arise until rudiment formation [37].

Asymmetric binding of thyroid hormones to gut cells is common to sea urchins, sea stars, and brittle stars. This may reflect the asymmetric development of adult structures in pre-metamorphic echinoderms. A greater quantity and intensity of the putative binding sites in the gut wall nearest the somatocoel suggests a potential shared mechanism of signaling from the gut wall to developing adult structures in the early rudiment. TH exposure resulted in acceleration of skeletogenesis in the rudiment,

(See figure on next page.)

Fig. 6 MAPK-P and T4-binding site distribution in *Pisaster ochraceus* gastrulae. Gastrulae were exposed for 90 min prior to fixation. Gastrulae were stained with Hoechst 33342 (blue; nuclei), rhodamine-conjugated T4 (red; T4-binding sites), and an antibody for phosphorylated MAPK (green, P-MAPK). **A** Maximum intensity projection of confocal fluorescent image of control *P.o.* gastrula. **B** Maximum intensity projection of confocal fluorescent image of gastrula exposed to T4 for 90 min. **C–C′** Focal slice of control gastrula showing tip of the archenteron and developing coelomic pouches. **D-D′** Focal slice of T4-exposed gastrula showing tip of the archenteron and developing coelomic pouches. MAPK phosphorylation patterns are similar to the control gastrula. Few to no T4-binding sites were observed in any early *P. ochraceus* gastrulae. **E** T4 did not significantly increase MAPK phosphorylation in *P.o.* gastrulae relative to the control. RGD peptide decreased MAPK phosphorylation relative to the control ($n = 5$, $p < 0.05$). Asterisk indicates significant difference from the control. **c**: Coelomic pouch, **ar**: Archenteron (gut)

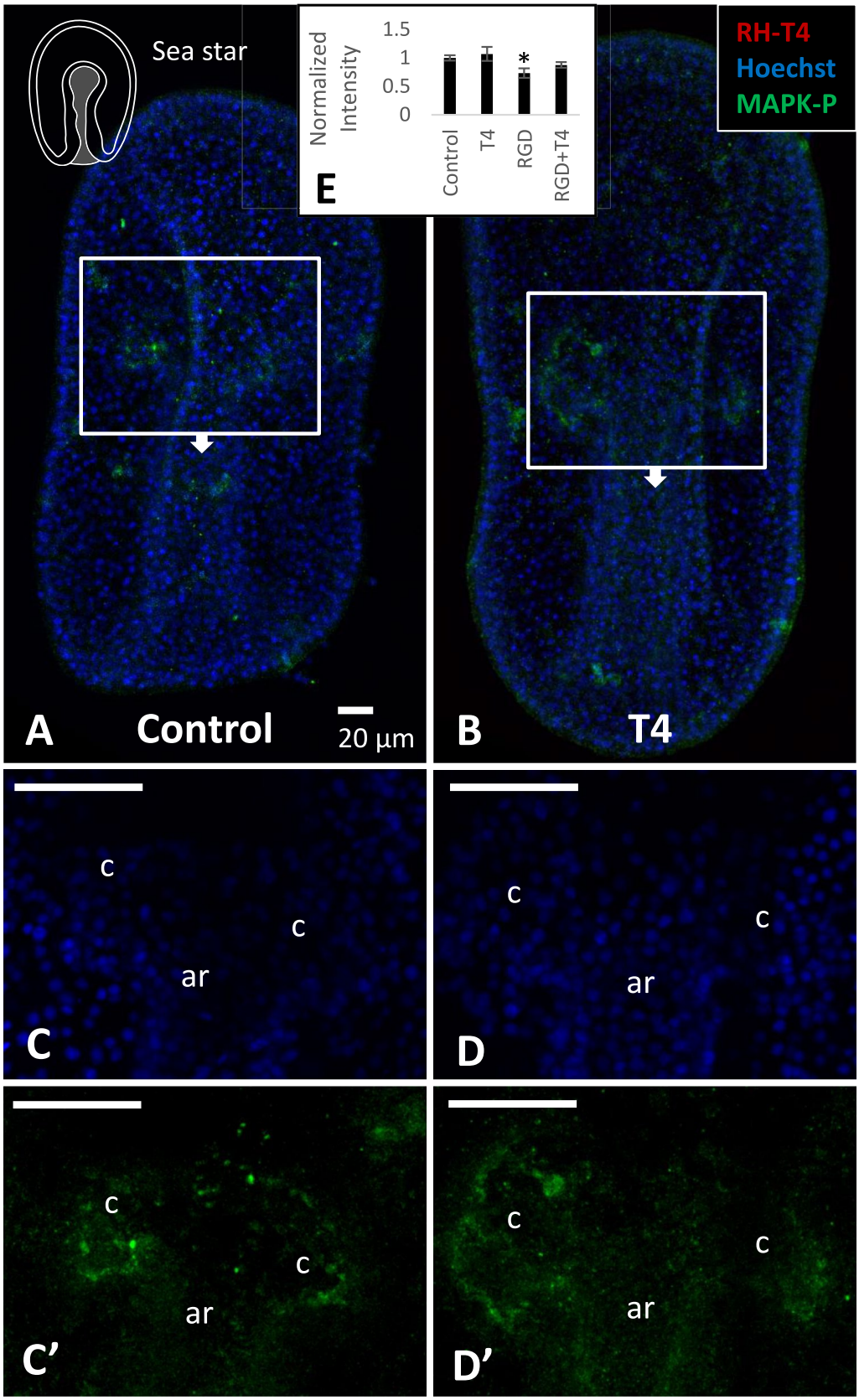

Fig. 6 (See legend on previous page.)

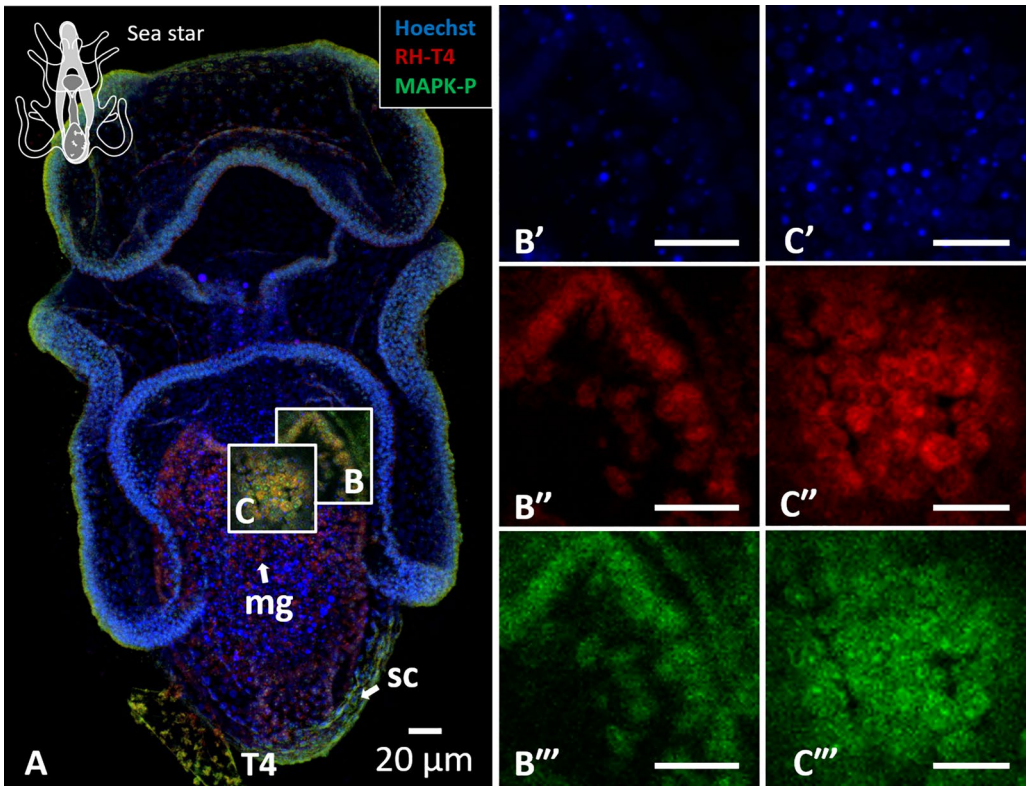

Fig. 7 MAPK and T4-binding site distribution in *Pisaster ochraceus* larva (bipinnaria). Larvae were exposed for 90 min prior to fixation. Bipinnaria was stained with Hoechst 33342 (blue; nuclei), rhodamine-conjugated T4 (red; T4-binding sites), and an antibody for phosphorylated MAPK (green, P-MAPK). **A** Maximum intensity projection of confocal fluorescent image of *P.o.* bipinnaria. **B-B‴** Focal slice of midgut wall. **C–C‴** Focal slice showing ventral view of midgut wall

a process blocked by inhibitors of TH binding to RGD-binding integrins. This provides preliminary evidence that TH signaling via a membrane integrin receptor in gut and rudiment cells may regulate skeletogenesis in adjacent mesenchyme.

Another possibility is that THs in the gut are binding to membrane transporters. Exogenous TH uptake has been proposed for echinoderms [29, 42, 74], and gut wall transporters would be a crucial element in exogenous hormone uptake [73]. The transporter hypothesis would partially explain why THs bind to some non-mesenchymal cells. These leave us with several explanatory hypotheses for this phenomenon: either THs are binding to transporters in the gut, or to receptors in the gut triggering release of a secondary signal (likely endocrine or neural, e.g., VEGF or serotonergic neuronal signaling).

The arrangement of sea urchin hydrocoel and somatocoel is also unique within echinoderms. Sea urchin hydrocoel is layered on the somatocoel, while in most echinoderms, the hydrocoel and somatocoel develop in distinct regions adjacent to the gut, with the hydrocoel developing proximal to the mouth region and the somatocoel developing closer to the midgut. In sea urchins, both somatocoel and hydrocoel develop adjacent to the midgut [98, 111]. This rearrangement of developing tissues in sea urchins may be related to the early skeletal development in the hydrocoel and the presence of TH-binding sites and acceleration of development of sea urchin hydrocoel by THs.

Sea urchin hydrocoel forms skeleton during rudiment development, but sea star and brittle star hydrocoel does not. Similarly, THs bind to sea urchin hydrocoel, particularly to the tips of the developing tube feet where skeleton will form. T4 shows little to no binding to sea star and brittle star hydrocoel. This suggests a possible link between TH receptor expression in sea urchin rudiment hydrocoel and TH regulation of skeletogenesis in sea urchin rudiment, which may be a synapomorphy of sea urchins relative to other echinoderms. In addition, T4 activates skeletogenesis in *P. ochraceus* before the coelomic sacs have wrapped around the gut, implying the source of skeletogenic cells is either migratory mesenchymal cells or gut cells, rather than the coelomic sac which will eventually form the hydrocoel.

Cocurullo et al. [16] provided circumstantial evidence based on transcriptional data that in sea urchin pluteus

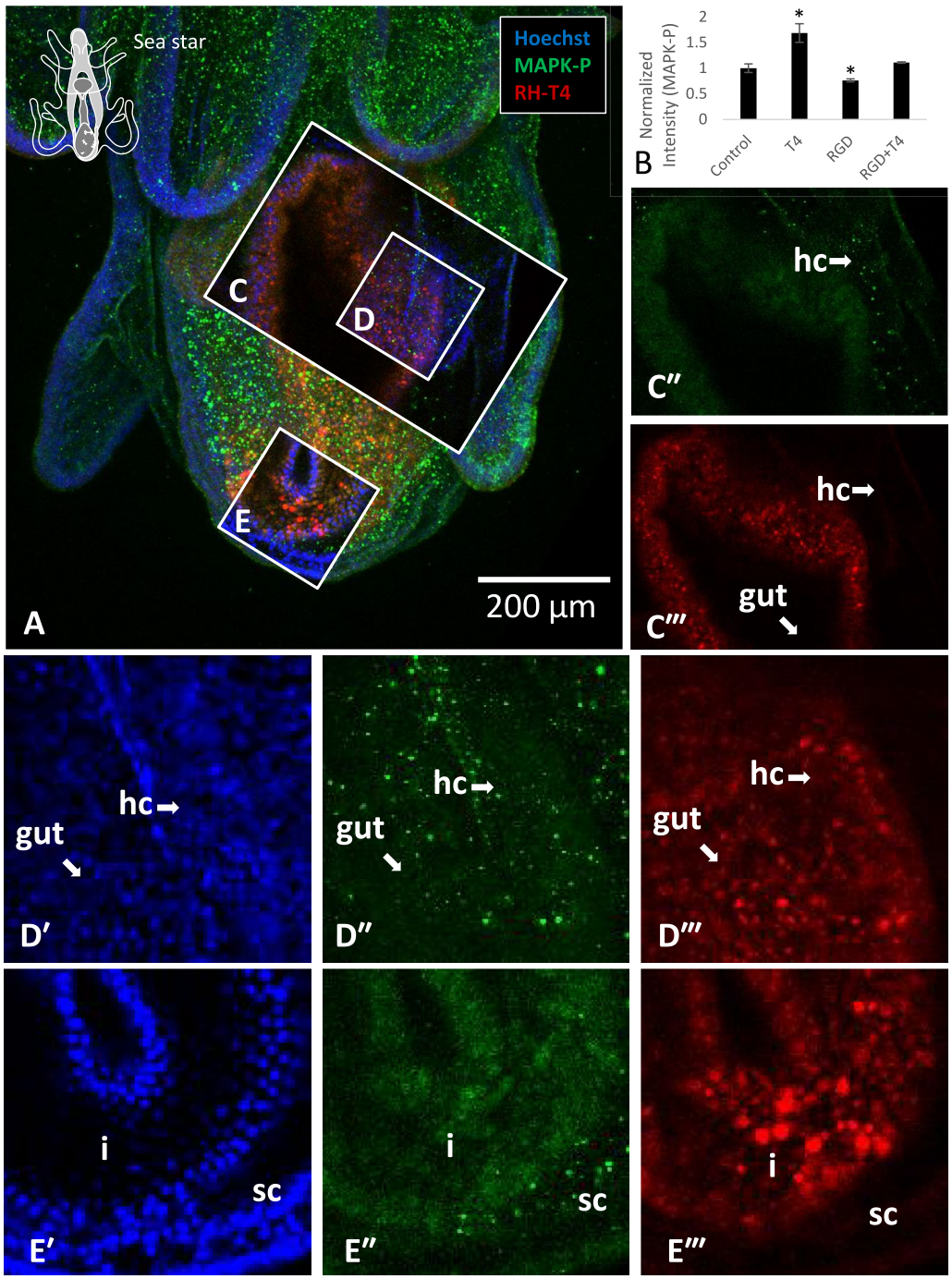

Fig. 8 MAPK and T4-binding site distribution in Pisaster ochraceus larva (brachiolaria) (A) Maximum intensity projection of a *Pisaster ochraceus* larva (brachiolaria) which has just begun rudiment development. Larvae were exposed for 90 min prior to fixation. **B** T4 increased MAPK phosphorylation in *P.o.* late bipinnaria/early brachiolaria relative to the control ($n=6$, $p<0.05$). RGD peptide decreased MAPK phosphorylation relative to the control ($n=6$, $p<0.05$). **C** Single slice of MAPK phosphorylation in midgut. **C′** Single slice of T4-binding locations in midgut. **D** Coelom adjacent to gut. **D′** MAPK phosphorylation in gut and coelom. **D″** T4-binding locations in gut. Coelom shows little T4-binding. **E** Nuclear stain of hindgut. **E′** MAPK phosphorylation in hindgut. **E″** T4-binding locations in hindgut. Asterisk indicates significant difference from the control. **hc**: hydrocoel, **gut**: midgut, **i**: intestine leading to anus, **sc**: somatocoel

larvae, THs may be synthesized in the gut and neurons proximal to the gut (putative TH synthesis enzymes colocalized with typical gut and neuronal markers). They found expression of peroxidasin and deiodinase (both are potentially involved in TH synthesis), putative TH transporters, and both THR and integrin membrane receptor in early pluteus larvae. We found that the putative TH synthesis enzymes were regulated by THs in pre-metamorphic sea urchin larvae [106]. This corresponds well with previous models in which THs were both exogenously and endogenously sourced, consumed as part of a typical algal diet and synthesized by iodinating dityrosine residues [29, 42]. In both cases, THs would be sourced proximal to the gut. Given the lack of a circulatory system and hypothalamic–pituitary–thyroid axis, we predicted that TH-binding sites in Echinoderm larvae might also be gut-proximal. As the juvenile rudiment is adjacent to the gut in species of Echinoderm which produce one, this would provide a plausible explanation for thyroid hormone regulation of development to metamorphosis, and settlement.

Evolution of skeletogenic gene regulation in echinoderms

While the gene regulatory network (GRN) underlying adult skeletogenesis is an apparent apomorphy shared by extant echinoderms, larval skeletogenesis is likely a synapomorphy of sea stars, brittle stars, and sea urchins (Fig. 1, [93]). A possible model for the evolution of echinoderm larval skeletogenesis is of a single transfer of the adult GRN to early larval echinoderm development, followed by a secondary loss of larval skeleton in sea stars, and partial loss in sea cucumbers [32]. Alternatively, multiple origins of skeletogenesis in Echinodermata have been proposed and this hypothesis remains under investigation [12, 28, 70].

MAPK phosphorylation of Ets1 is responsible for the majority of MAPK effects in skeletogenic sea urchin mesenchyme [93], and a MAPK cascade phosphorylating Ets1 is necessary for skeletogenesis in sea urchin larvae [34, 56, 85, 88]. During skeletogenesis, MAPK phosphorylates Ets1, leading to activation and increased transcription of *alx1*, followed by expression and activation of skeletogenic products. For echinoderm skeletogenesis to occur, three elements are necessary: (1) a source of MAPK/ERK signal activation, (2) Ets1 phosphorylation, (3) *alx1* expression. Ancestrally, *ets1* likely specified both adult skeleton and larval mesoderm in echinoderms [60]. Previously, T4 has been found to upregulate *ets1* in sea urchin gastrulae (qPCR; [104]), as well as a complement of other skeletogenesis-related genes (RNA-seq; Taylor & Heyland, 2023). However, it is still unclear whether TH acceleration of skeletogenesis acts primarily via phosphorylation or upregulation of key transcription factors or downstream effector genes.

Our results from this study confirm previous work on MAPK activation via THs in sea urchins [104] and provide new evidence for this mechanism in sea stars, and brittle stars. These findings support the hypothesis that an integrin receptor binding THs and capable of MAPK signal transduction is a common feature of echinoderm skeletogenic mesenchyme. Recent work further supports this hypothesis, as T4 and to a lesser extent T3 bind to membrane fractions of sea urchin embryos [106]. However, limited efficacy of PD98059 in blocking skeletogenesis at some stages suggests that MAPK signaling may not be entirely necessary for skeletogenesis, only sufficient. Alternatively, an increased concentration of PD98059 as was used in Taylor and Heyland [104] may have inhibited skeletogenesis more fully.

We additionally found that RGD peptide inhibited the action of THs. A putative RGD-binding integrin which is a likely candidate for TH binding (Integrin αPβG) has been reported to have high expression in sea urchin gastrula PMCs, the skeletogenic cells during early sea urchin development [16, 69, 101] and also the cells in which we find the greatest influence of T4 on MAPK phosphorylation. In ophioplutei, mesenchymal cells adhered to the skeleton also showed a MAPK phosphorylation response

(See figure on next page.)

Fig. 9 Thyroid hormones bind and increase MAPK phosphorylation in the somatocoel and in presumptive skeletogenic mesenchyme in the larval arms in *O. aculeata*. Larvae were exposed for 90 min prior to fixation. **A, B** Maximum intensity projection of *Ophiopholis aculeata* larvae (ophiopluteus) after T4 exposure. Larva A is in the early stages of metamorphic development (**Stage 0** per our scheme). Larva B is in **Stage 2**, possessing a five-lobed hydrocoel. **C–C″′** Single focal slice revealing T4-binding locations and MAPK phosphorylation in a larval arm. Arrowheads (▶) indicate presumptive skeletogenic mesenchyme. **D-D″′** Single focal slice showing 5-lobed hydrocoel. Arrowheads (▶) indicate hydrocoel lobes. Little to no T4 binding is detected in the hydrocoel and hydrocoel MAPK phosphorylation does not differ from control larvae. **E-E″′** Single focal slice showing somatocoel adjacent to the gut. Regions of increased T4 binding and MAPK phosphorylation are indicated with arrowheads (▶). T4-binding cells, indicated with arrowheads (▶), do not present with greatly increased MAPK phosphorylation. **hc**: hydrocoel, **gut**: midgut, **sc**: somatocoel, **la**: larval arm. **F** T4 binds primarily to the midgut and presumptive skeletogenic mesenchyme cells in ophiuroid larvae ($n=4$, $p<0.05$, significant differences exist between cell types with no shared letter). We observed little binding in the ciliated bands and epithelial tissues, with some observed binding in the hydrocoel and posterior coelom/somatocoel. **G** T4 increases MAPK intensity in O. a. larvae ($n=4$, $p<0.05$). This effect may be partially inhibited by RGD peptide ($n=4$, $p>0.05$)

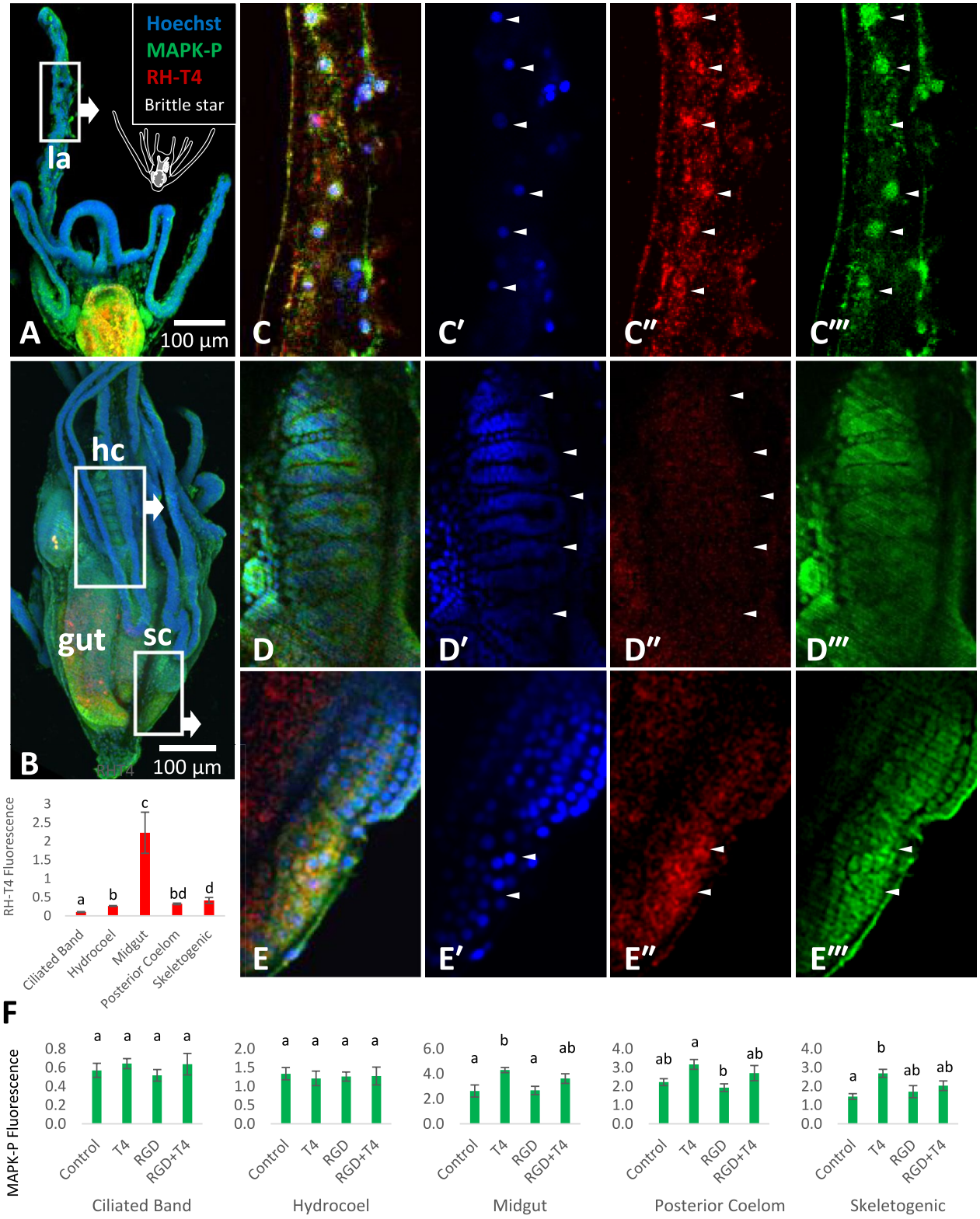

Fig. 9 (See legend on previous page.)

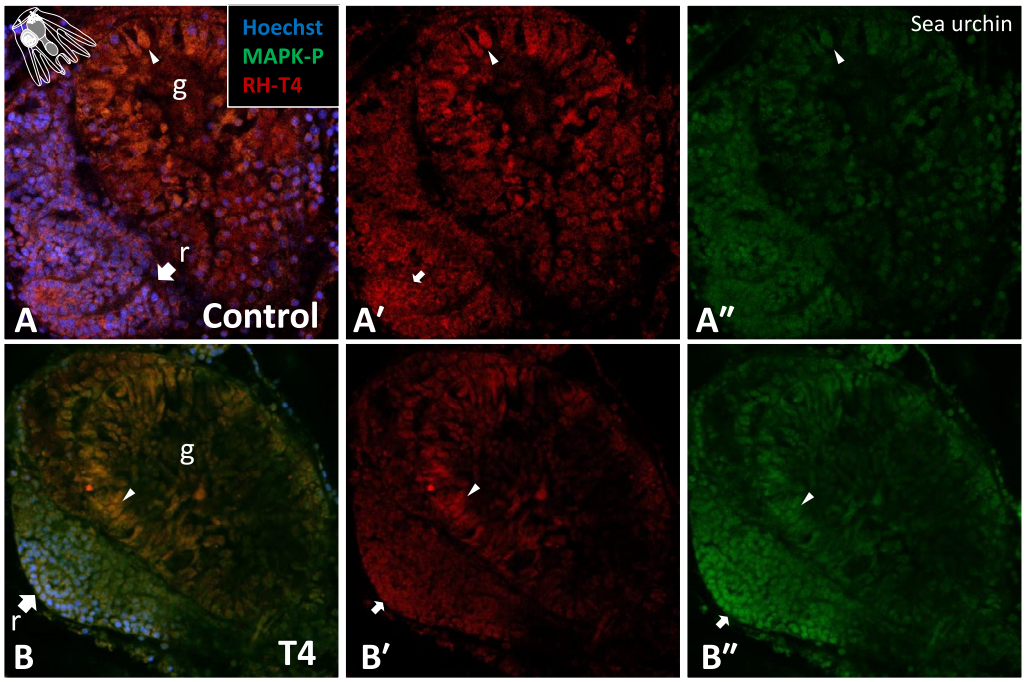

Fig. 10 T4 binds to gut and rudiment in *S. purpuratus* larvae. Exposure to T4 increases MAPK phosphorylation in the midgut and rudiment. Larvae were exposed for 90 min prior to fixation. Larvae were stained with Hoechst 33342 (blue; nuclei), rhodamine-conjugated T4 (red; T4-binding sites), and an antibody for phosphorylated MAPK (green, P-MAPK). Exposure to T4 and RGD peptide increases binding locations for T4 in the midgut. **A** Control larva. Demonstrates binding sites for T4 in the gut and rudiment cytoplasm/membrane. Arrowhead (▶) indicates an example of a T4-binding site in gut. Arrow indicates T4 binding in rudiment. **A′** T4-binding locations in control larva. **A′′** MAPK phosphorylation locations in control larva. Overall MAPK phosphorylation is low and primarily limited to the growth regions at the tip of the rudiment and some gut cells. **B** T4-exposed larva. **B′** T4-binding locations in gut and rudiment. Arrowhead (▶) indicates an example of a T4-binding site in gut. Arrow indicates T4 binding in rudiment. **B′′** MAPK phosphorylation in gut and rudiment. Arrow (➡) indicates region of greatest phosphorylation in rudiment, at the tips of the developing lobes

to TH exposure, suggesting that ophiuroid skeletogenic mesenchyme may also be expressing a TH/RGD-binding integrin.

At the concentration we used, RGD alone has no detectable effects on skeletogenesis. If RGD was affecting skeletogenesis by altering PMC adhesion, we would expect to see a decrease in spicule deposition rate of RGD-exposed larvae. We have not seen this, either in this manuscript, or in previous work [102, 104]. While this evidence suggests an inhibitory effect of RGD peptide on TH binding and activity, RGD peptides may also have additional signaling effects. For instance, we observed RGD inducing whole-body muscular contractions in sea star larvae. As well, we saw a small, but statistically significant effect of RGD peptide on MAPK levels in sea star larvae, and previous work showed an effect of extremely high concentrations of RGD peptide (10 μM) on initiation of skeletogenesis in previous work [104].

Expression of RGD-binding proteins is crucial for epithelial–mesenchyme transition in echinoderms [40, 55], vertebrates [31, 66, 77], and non-bilaterians [67], and may predate multicellular life [20]. RGD-binding of integrins to an extracellular matrix allows for selective adhesion, detection of the ECM, and signal transduction, which may have contributed to the evolution of multicellularity. Sponges and corals—some of the earliest branching metazoans—utilize iodinated tyrosine residues in the construction of the skeletal matrix, which in some sponges and corals is composed of up to 10–26% iodine (dry weight), predominantly in the form of iodinated scleroproteins [38, 87]. The greatest fraction of the iodinated tyrosine is in the form of T2 and T4 [78, 87] with exposure to T4 increasing the skeletal deposition rate in corals [57, 78]. It is, therefore, conceivable that thyroid hormones served as a structural element of early metazoan ECM. It is not clear whether T4 in corals has a regulatory effect, or if increased skeletal deposition rate as a result of T4 exposure is a consequence of increased material availability. In contrast, the primary active form of THs in vertebrates, T3, has not been detected in non-bilaterians [87, 102]. We speculate that the capability of RGD-binding integrins to bind T4 and other iodinated tyrosine compounds may have an ancient origin in non-bilaterians (discussed in [103]), though the mechanism

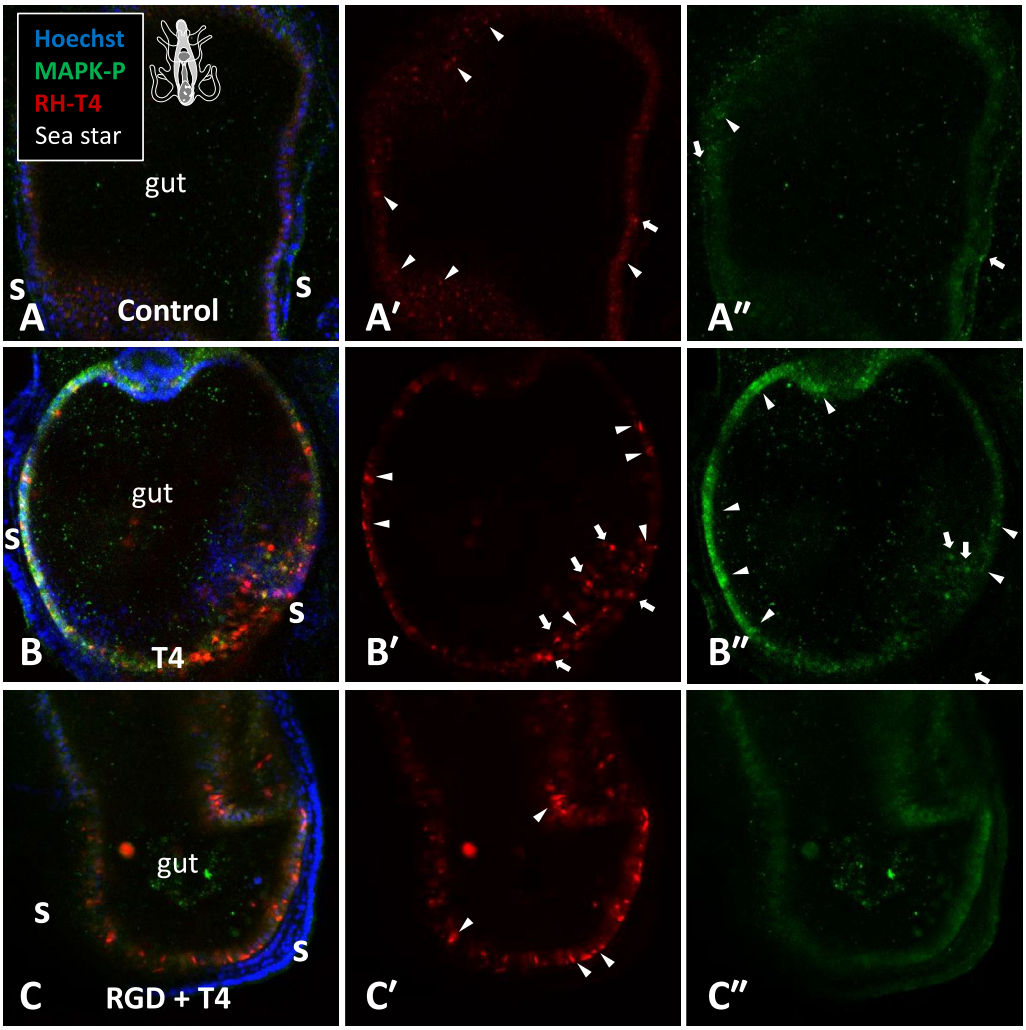

Fig. 11 RGD inhibits the effect of T4 in *Pisaster ochraceus* larvae. T4 binds to gut and somatocoel in *P. o.* larvae. Larvae were exposed for 90 min prior to fixation. Exposure to T4 increases MAPK phosphorylation in the midgut and somatocoel. Larvae were stained with Hoechst 33342 (blue; nuclei), rhodamine-conjugated T4 (red; T4-binding sites), and an antibody for phosphorylated MAPK (green, P-MAPK). Exposure to T4 and RGD peptide increases binding locations for T4 in the midgut. Arrowheads (▶) indicate T4 binding or MAPK phosphorylation in the gut wall. Arrows indicate T4 binding or MAPK phosphorylation outside the gut wall. **A-A′′** Control larva, from left to right: Combined image, T4-binding sites, MAPK phosphorylation. T4-binding locations are visible in and adjacent to the gut. **B-B′′** T4-exposed larva, from left to right: Combined image, T4-binding sites, MAPK phosphorylation. T4-binding locations are visible in and adjacent to the gut, especially adjacent to the somatocoel. Regions of increased MAPK phosphorylation correspond roughly with T4-binding sites. **C–C′′** RGD and T4-exposed larva, from left to right: Combined image, T4-binding sites, MAPK phosphorylation. T4-binding sites are present in the gut wall, but effects of T4 on MAPK phosphorylation are reduced. There is an increase of T4-binding sites in RGD-exposed larvae. **s:** Somatocoel. **Gut:** midgut

of action and function of T4 in non-bilaterians remains unknown.

Echinoderms possess a single THR gene, orthologous to THRβ, and while binding of THs to the echinoderm THR has not been demonstrated, we have previously shown that T4 can regulate gene expression of genes proximal to TH response elements in the genome [106]. Furthermore, T4 can bind to nuclear extract from echinoid cells [92]. Our results here show TH binding to the nucleus in sea star and sea urchin gut and rudiment. We only observed this binding in late-stage larvae, corroborating our previous hypothesis that T4 regulation of gene expression via THR is a late-larval phenomenon in sea urchins [106]. In this study, T4 exposure resulted in an increase of TH-binding locations, an effect which was not inhibited by RGD peptide in sea urchin, ophiuroids and sea star larvae. Autoregulation of the THR is a classic sign of canonical TH signaling via a nuclear receptor, an effect which we also detected in Taylor et al. [106]. Since RGD is not known to bind to the nuclear hormone

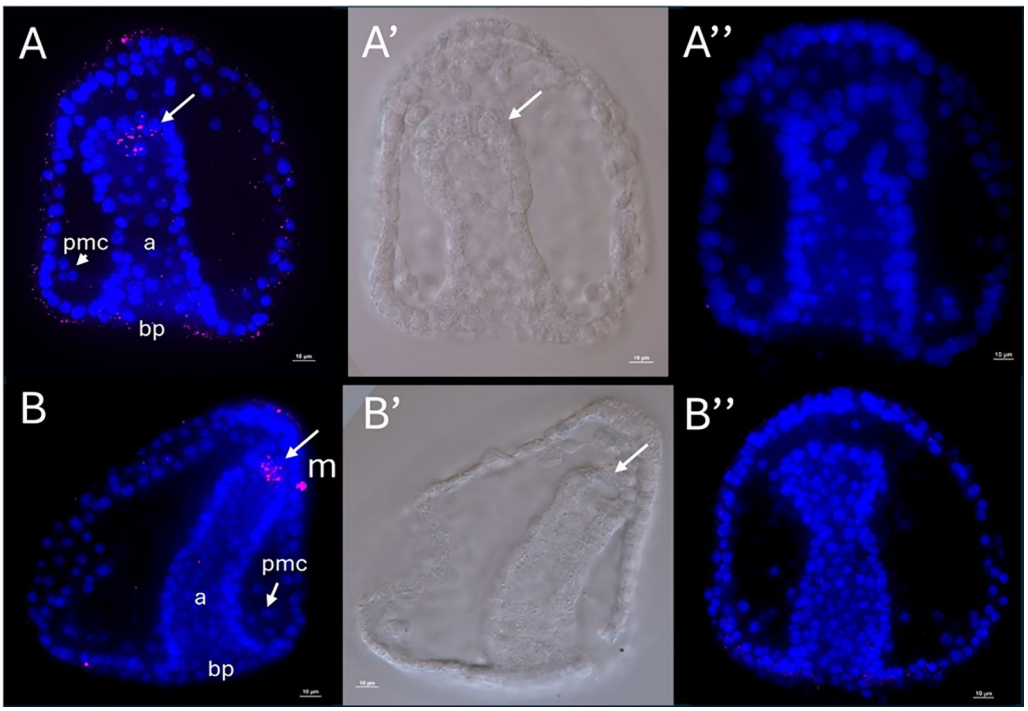

Fig. 12 Immunohistochemistry using a monoclonal thyroxine antibody reveals localization of thyroxine positive cells at the tip of the developing archenteron and mouth. **A** Maximum Z-projection of gastrulating sea urchin embryo 40 hpf, showing thyroxine positive cells at the tip of the archenteron, **A'** representative optical section in DIC showing some of the cells stained, **A"** negative control with pre-absorbed thyroxine antibody of stage-matched embryo shows no staining. **B** Maximum Z-projection of gastrulating sea urchin embryo 48.5 hpf, showing thyroxine positive cells at the tip of the archenteron and mouth. **B'** representative optical section in DIC showing some of the cells stained, **B"** negative control with pre-absorbed thyroxine antibody of stage-matched embryo shows no staining. Scale bar: 10 µm. Pmc: Primary mesenchyme cells, bp: blastopore, a: archenteron, arrow points to positive staining

receptor, this suggests that expression of TH-binding locations may be under control of a non-integrin mechanism, such as via autoregulation by the THR, providing evidence for canonical TH signaling activity in all three classes of Echinoderm we examined.

The commonality of binding locations and the evidence that THs may regulate metamorphic development in echinoids [15, 44, 91] and sea stars [54] suggests a potential role for THR in regulating echinoderm metamorphosis. However, unpublished data mentioned by Holzer et al. [48] suggests that T4, among other TH compounds, may not bind to sea star isolated THR, and these authors hypothesized that THR may be functioning while unliganded. In addition, it appears that retinoic acid signaling via the retinoic acid receptor (RAR) instead may be a mechanism for nuclear hormone receptor-regulated metamorphosis of sea stars, as in crinoids [115, 116]. Evidence for genomic regulation of development by THs by binding to a THR is strong in sea urchins and tenuous for sea stars and brittle stars. Future research will have to test this hypothesis further by analyzing transcriptomic response to THs (as in [106]), ideally with a ChIP assay or binding kinetics to confirm TH binding to THR.

Thyroid hormone signaling has been repeatedly co-opted to regulate developmental processes. Not only do THs work via multiple independently evolved mechanisms [25], THs regulate developmental processes which also evolved independently. For example, THs appear to regulate skeletogenesis in both echinoderms and chordates—but echinoderm skeletogenesis is a novelty of the phylum and distinct in both regulatory mechanisms and material components from chordate skeletogenesis [2, 64, 76, 85]. THs additionally regulate metamorphic development or settlement in molluscs, annelids, echinoderms, and chordates [11, 15, 36, 44, 47, 49, 53, 58, 79, 80, 91], a process which may or may not share a single origin. As well, THs regulate diverse other developmental systems, including neurogenesis, vasculogenesis, metabolism, and myogenesis [7, 25]. THR actions rely on RXR, a transcription factor which is already implicated in a large number of transcriptional regulatory events [33] and creates a signaling complex with THR in at least insects and vertebrates. The genomic TH mechanism has the ability to activate and regulate numerous genes [106, 109] and RXR is ubiquitously expressed [33, 108], meaning coexpression

of THR and TH availability are the main regulators of cell responsiveness to THs via the genomic pathway. Synthesis and metabolism of THs is common to most metazoans, with most animals having the ability to synthesize thyroxine and other THs [103]. Nuclear hormone receptor heterodimers with RXR as a component are implicated in control of development and metamorphosis in metazoans [39, 62], including cnidarians which do not possess a THR [35]. These features combined create a readily evolvable system of TH gene regulation. Similarly, non-genomic signaling acts via integrin activation of MAPK, a ubiquitous pathway which can be triggered by a commonly expressed class of proteins: RGD-binding integrins [3, 17, 25, 102, 104]. Receptiveness to integrin-mediated signaling can easily evolve in multiple cell types, relying only on proximity to a source of THs and expression of a TH-binding integrin making TH signaling a versatile system in both development and evolution. In a cell containing both signaling pathways, we speculate that external THs would first activate the integrin signaling pathway, triggering rapid phosphorylation and activation of proteins (including the nuclear THR) before being transported to the cytoplasm/nucleus and binding to the nuclear THR to regulate gene transcription.

Thyroid hormone regulation of skeletogenic mesenchyme appears to be a common mechanism in echinoderms, including conserved expression of an integrin receptive to T4 which can trigger a MAPK cascade, and a conserved requirement for a MAPK cascade phosphorylating Ets1 and initiating skeletogenesis via Alx1 [21, 37, 59, 70, 88]. Skeletogenesis is an essential component of metamorphic development and acceleration of skeletogenesis may play a role in regulation of metamorphosis, particularly in echinoid larvae [41, 81, 104, 112]. TH levels in sea urchins rise prior to metamorphosis [15], contributing to the control of developmental timing of metamorphosis and settlement. The acceleration of skeletogenesis by THs represents an extremely evolvable mechanism, as THs would already be present in and proximal to the rudiment, and skeletogenic mesenchyme would already be sensitive to MAPK phosphorylation. MAPK regulation of skeletogenic activity seems to be present in all echinoderms. The only necessary element would be expression of a TH-binding integrin to trigger or enhance MAPK signaling. TH regulation of skeletogenesis appears to exist in sea urchins, sea stars, and brittle stars. Alternatively, the inverse could apply: TH regulation of metamorphosis would be extremely evolvable in the case that THs are already synthesized or transported to the rudiment to control skeletogenesis. THs accelerate both larval and adult skeletogenesis in larval brittle stars and sea urchins (and adult skeletogenesis in sea star larvae). It seems increasingly likely that TH regulation of echinoderm skeletogenesis is at least as ancient as the divergence of Echinozoa and Asterozoa.

Critically, the hypothesis that endogenous hormone synthesis is responsible for regulation of skeletogenesis in larval and adult echinoderms is still mostly untested. Previous work with inhibitors of endogenous TH synthesis demonstrated that endogenous TH synthesis is relevant for development in sea urchins [4, 15, 43, 44, 89]. TH mechanisms in echinoid metamorphic development may involve peroxidase-facilitated diffusion or transport [43, 74]. For the first time, we showed thyroxine presence in specific sea urchin embryonic cells. We identified several thyroxine positive cells at the tip of the developing archenteron and sea urchin gastrulae. These cells are located in the region of the pharyngeal endoderm and are located in proximity to endoderm derived neurons previously described [110]. While similar in origin to endostyle-derived cells in urochordates and cephalochordates, the cell lineage giving rise to these cells will require further investigation. Coinciding with our results, gene expression of putative TH synthesis genes has also been shown in gastrulae [16], particularly in gut-proximal neurons and gut cells.

In addition, responsiveness to THs in echinoderm gastrulae may be a consequence of a shared GRN in gastrulae, larvae, and adults, and not a trait which is active under normal physiological conditions. Future work should focus on inhibition of TH synthesis and attempt to determine which effects of THs, if any, are derived from endogenous hormone synthesis versus exogenous hormone sources (as in the vitamone hypothesis; [29]), as well as the source of thyroid hormones in Echinoderm embryos and larvae.

Skeletal loss/reduction in sea stars and sea cucumbers

In the case of a single larval origin of skeletogenesis, there is currently no satisfactory explanation for the loss of skeleton in sea star larvae. Sea cucumbers and sea stars have likely undergone an independent loss of larval skeleton in comparison to sea urchins and brittle stars. The reduction in sea cucumber larval skeleton might be attributed to the same evolutionary process as the reduction in adult skeleton, given that they share a GRN [70, 118], and expression of biomineralization-related genes is greatly reduced in the adult [97, 118]. It is possible that the adult skeleton of sea stars has also been reduced, as they possess less skeleton (dry weight) than either sea urchins or brittle stars [27]. The adult skeleton is highly reduced in sea cucumbers, some crinoids, and some extinct echinoderms [95–97, 117]. In contrast with sea star larvae, sea cucumbers still initiate larval skeletogenesis and have larval skeletogenic mesenchyme. It is likely

that the sea cucumber larval skeleton was reduced from an ancestral state, given the close relation to sea urchins and brittle stars, both of which have extensive larval skeletons. It has been suggested that sea cucumber adult skeletal reduction is an example of paedomorphosis [19, 95]; however, it is not clear whether reduction in larval or adult skeletogenesis came first, or if due to the shared regulatory mechanism, the reduction was simultaneous. The secondary reduction in sea cucumber skeleton appears to be a likely result of modification or loss of transcription factors in the skeletogenic mesenchyme, possibly related to the reduction in adult skeleton. This contrasts with reduced sea star skeleton which relies on non-expression of the skeletogenic transcription factors until metamorphic development. For this reason, we hypothesize that sea cucumber larvae may still be responsive to thyroid hormone exposure and predict that they might undergo accelerated or expanded skeletogenesis after TH exposure. This could be tested in future experiments and would shed light on both sea star and sea cucumber skeletogenesis, as well as the differing evolutionary trajectories that led to reduction/loss of larval skeletogenesis in both lineages.

Sea star larvae do not express *alx1* and are, therefore, incapable of producing skeleton until metamorphic development when coelom-derived mesenchyme likely becomes primed for skeletogenesis by expressing *alx1* and other skeletogenic regulatory genes [59]. In contrast, sea cucumbers retain expression of *alx1*, but have lost expression of downstream secondary transcription factors in the skeletal mesenchyme [70]. This explains why sea star gastrulae were unresponsive to THs in our experiments: Alx1 is not present to be phosphorylated, and therefore, no skeleton can be formed [59]. The full complement of skeletogenic regulator genes is present and functional in sea stars, but not expressed in larval cells until the production of skeleton in the rudiment prior to metamorphosis. This may represent a secondary loss of the previously evolved heterochronic activation of the skeletogenesis program during larval gastrulation [93].

Thyroid hormone regulation of developmental timing

Regulation of developmental timing is critically important in the case of both larval and juvenile skeletogenesis. Larval skeleton in sea urchins and brittle stars supports the larval arms which act as both feeding structures and a defense against predation [5, 99]. Skeletogenesis must begin soon after hatching, as the larvae prepare to feed. In late-stage larvae, development to metamorphosis and juvenile skeletogenesis are essential steps to prepare for life on the benthos. *P. ochraceus* can produce skeleton weeks before metamorphosis [83]. *S. purpuratus* develops skeletal elements 5–7 days prior to metamorphosis, and *O. aculeata* produces skeleton only 1 or 2 days before metamorphosis. These represent differing strategies of resource investment in juvenile structures during the larval feeding stage. Control of resource allocation towards metamorphic development must be carefully balanced with larval growth [99]. For instance, in sea urchins, THs increase skeletogenesis in the juvenile rudiment while shortening the larval arms [1, 15, 44, 113]. Similarly, THs may allow for control of resource investment in both brittle star and sea star larvae. One potential source of THs is exogenous [29, 42], implying that food availability might modulate late-larval development.

P. ochraceus is also notable for spending a longer than typical time developing juvenile structures as a brachiolaria larva [83]. The early responsiveness of *P. ochraceus* skeletogenesis to THs may relate to the need for temporal control of the extended development to metamorphosis. In contrast, *O. aculeata* develops few skeletal structures prior to a rapid metamorphosis and was only responsive to TH acceleration of juvenile skeletogenesis several days before a typical metamorphosis would occur.

We did not examine any direct-developing echinoderms (echinoderms which develop directly from egg to adult without a feeding larval stage). Echinoderm eggs are maternally provisioned with THs [15] and TH regulation of metamorphic development is sufficient to allow an obligate feeding species with an indirect development to act as a facultative feeding larva and metamorphose without the need for food [44], albeit with a much smaller juvenile size. Based on the potentially shared mechanisms and role of THs in sea stars and brittle stars, we predict that the same phenomenon might be observed in non-echinoid echinoderms.

Conclusions

Thyroid hormones, principally thyroxine, accelerate initiation of skeletogenesis in sea urchins, sea stars, and brittle star larvae. THs also accelerate initiation of skeletogenesis in brittle star and sea urchin gastrulae, but do not induce ectopic skeletogenesis in sea star gastrulae (which normally do not produce skeleton). Thyroid hormones bind to cells proximal to regions of skeletogenesis, primarily in the gut and rudiment, and stimulate MAPK phosphorylation. We found putative T4-binding sites in the nucleus, cytoplasm, and membrane, depending on the larval stage and echinoderm, with nuclear binding being most prominent in sea urchin gastrulae, as well as the gut/rudiment of late-stage sea urchin, brittle star, and sea star larvae. RGD peptide, an inhibitor of the RGD-binding pocket in RGD-binding integrins, inhibits the effect of thyroid hormones in all three echinoderm classes examined. PD98059, an inhibitor of MAPK signaling, prevents the

effect of THs on skeletogenesis, especially in sea star larvae, but had little effect alone at the concentration used. Thyroid hormones may act non-genomically, via a membrane integrin receptor-mediated MAPK cascade in sea stars, brittle stars, and sea urchins. TH regulation of mesenchyme cell activity may be an ancient mechanism to control timing of development, including skeletogenesis. TH regulation of skeletogenesis in late mesenchyme cells prior to metamorphosis may have been co-opted to regulate larval skeletogenesis in sea urchins and brittle stars.

Supplementary Information

The online version contains supplementary material available at https://doi.org/10.1186/s13227-024-00226-2.

Additional file 1: Figure S1. MAPK quantification methods. (A) MAPK phosphorylation was quantified by automatic cell counting in the Hoechst 33342 channel (1; Hoechst), followed by thresholding (2; Hoechst), identification of nuclei locations (3; Hoechst), pruning nuclei which were more centered on another stack slice (4; Hoechst), and measurement of fluorescent intensity of each individual cell in a radius around each nucleus (5 [RHT4], 6 [MAPK-P) (see file S1. for ImageJ script). (B) Intensity was normalized to the Hoechst 33342 signal to account for attenuation.

Additional file 2: Figure S2. RGD effects on muscle contraction in *Pisaster ochraceus*. RGD peptide induced repeated whole-body muscle contractions in *P. ochraceus* bipinnaria. This effect was observed to a lesser degree in brachiolaria.

Additional file 3: Figure S3. MAPK and T4-binding site distribution in *Dendraster excentricus* gastrula exposed to T4. Gastrula was exposed to 10^{-7} M T4 for 90 minutes. Gastrula was stained with Hoechst 33342 (blue; nuclei), rhodamine-conjugated T4 (red; T4-binding sites), and an antibody for phosphorylated MAPK (green, P-MAPK). Both T4-binding sites and MAPK activation are ubiquitous during early gastrulation. (A) Maximum intensity projection of confocal fluorescent image of *D.e.* gastrula, 30 hours post-fertilization. (B) Close-up side view of lateral ectoderm. (C) Close-up of extracellular matrix and basal membrane near ventrolateral cluster (vlc). T4 binds clearly to the nucleus-proximal membrane. (D) Nucleus and cytoplasm of cells near ventrolateral cluster. T4 shows strong nuclear and perinuclear binding.

Additional file 4: Figure S4. Ectopic skeleton and accelerated skeletogenesis in *Dendraster excentricus*. (A) Whole-larva view of skeleton. Additional skeleton was observed in the larval arms and posterior end. (B) Ectopic arm skeleton formed duplicate parallel larval arms, connected with a "window-like" network. (C) Ectopic skeleton at the posterior end formed a network reminiscent of late-larval development, similar to a juvenile plate. Curled arrow indicates that this is a posterior view of the same larva. (D) Larvae were exposed to the thyroid hormones, rT3, T3, and T4 (10^{-7} M), RGD peptide (RGD; 10^{-7} M) or PD98059 (PD; $5x10^{-7}$ M). Thyroid hormones, including T4 and T3, accelerate initiation of skeletogenesis in. RGD peptide and PD98059 inhibit the effects of THs on skeletogenesis (t-test, $p < 0.05$).

Additional file 5: Figure S5. Hormone exposure methods (A) Schematic diagram of fluorescence microscopy methodology. (B) Schematic diagram of late-larval exposure methodology. (C) Schematic diagram of gastrula exposure methodology.

Acknowledgements
We would like to acknowledge Jonathan D. Allen, Sophie B. George for providing embryos and larvae, as well as Friday Harbor Laboratories.

Author contributions
E.T. and A.H. contributed to the initial conception, design, interpretation, and revisions of this manuscript. A.H. and M.C. designed, imaged, and analyzed the work depicted in Figure 12. E.T. wrote the initial manuscript draft, conducted the experiments, and analyzed the data in Figures 1-11.

Funding
All research described here was supported by NSERC Discovery Grant 400230 to AH.

Data availability
Not available.

Declarations

Competing interests
The authors declare no competing interests.

Received: 12 January 2024 Accepted: 22 May 2024
Published online: 07 August 2024

References

1. Armstrong AF, Lessios HA. The evolution of larval developmental mode: Insights from hybrids between species with obligately and facultatively planktotrophic larvae. Evol Dev. 2015;17(5):278–88. https://doi.org/10.1111/ede.12133.
2. de-Leon SB-T. The Evolution of Biomineralization through the Co-Option of Organic Scaffold Forming Networks. Cells. 2022;11(4):595. https://doi.org/10.3390/cells11040595.
3. Bergh JJ, Lin H-Y, Lansing L, Mohamed SN, Davis FB, Mousa S, Davis PJ. Integrin αVβ3 Contains a Cell Surface Receptor Site for Thyroid Hormone that Is Linked to Activation of Mitogen-Activated Protein Kinase and Induction of Angiogenesis. Endocrinology. 2005;146(7):2864–71. https://doi.org/10.1210/en.2005-0102.
4. Bevelander G. Effect of thiourea on development of the sea urchin arbacia punctulata. Proc Soc Exp Biol Med. 1946;61(3):268–70. https://doi.org/10.3181/00379727-61-15297.
5. Boidron-Metairon IF. Morphological plasticity in laboratory-reared echinoplutei of Dendraster excentricus (Eschscholtz) and Lytechinus variegatus (Lamarck) in response to food conditions. J Exp Mar Biol Ecol. 1988;119(1):31–41. https://doi.org/10.1016/0022-0981(88)90150-5.
6. Bolte S, Cordelières FP. A guided tour into subcellular colocalization analysis in light microscopy. J Microsc. 2006;224(3):213–32. https://doi.org/10.1111/j.1365-2818.2006.01706.x.
7. Brent GA. Mechanisms of thyroid hormone action. J Clin Investig. 2012;122(9):3035–43. https://doi.org/10.1172/JCI60047.
8. Brtko J. Thyroid hormone and thyroid hormone nuclear receptors: History and present state of art. Endocr Regul. 2021;55(2):103–19. https://doi.org/10.2478/enr-2021-0012.
9. Cannon JT, Kocot KM, Waits DS, Weese DA, Swalla BJ, Santos SR, Halanych KM. Phylogenomic resolution of the hemichordate and echinoderm clade. Curr Biol. 2014;24(23):2827–32. https://doi.org/10.1016/j.cub.2014.10.016.
10. Carpizo-Ituarte E. L-Thyroxine induces metamorphosis in two species of marine gastropods. Am Zool. 1993;33:41A.
11. Carpizo-Ituarte E, Rosa-Velez JD. L-Thyroxine induces metamorphosis in two species of marine gastropods. Am Zool. 1993;33:41A.
12. Cary GA, Hinman VF. Echinoderm development and evolution in the post-genomic era. Dev Biol. 2017;427(2):203–11. https://doi.org/10.1016/j.ydbio.2017.02.003.
13. Cheng S, Eberhardt NL, Robbins J, Baxter JD, Pastan I. Fluorescent rhodamine-labeled thyroid hormone derivatives: Synthesis and binding to the thyroid hormone nuclear receptor. FEBS Lett. 1979;100(1):113–6. https://doi.org/10.1016/0014-5793(79)81143-6.
14. Cheng SY, Maxfield FR, Robbins J, Willingham MC, Pastan IH. Receptor-mediated uptake of 3,3',5-triiodo-L-thyronine by cultured fibroblasts. Proc Natl Acad Sci. 1980;77(6):3425–9. https://doi.org/10.1073/pnas.77.6.3425.

15. Chino Y, Saito M, Yamasu K, Suyemitsu T, Ishihara K. Formation of the Adult Rudiment of Sea Urchins Is Influenced by Thyroid Hormones. Dev Biol. 1994;161(1):1–11. https://doi.org/10.1006/dbio.1994.1001.
16. Cocurullo M, Paganos P, Wood NJ, Arnone MI, Oliveri P. Molecular and cellular characterization of the TH pathway in the Sea urchin strongylocentrotus purpuratus. Cells. 2023. https://doi.org/10.3390/cells12020272.
17. Cody V, Davis PJ, Davis FB. Molecular modeling of the thyroid hormone interactions with αvβ3 integrin. Steroids. 2007;72(2):165–70. https://doi.org/10.1016/j.steroids.2006.11.008.
18. Cohen K, Flint N, Shalev S, Erez D, Baharal T, Davis PJ, Hercbergs A, Ellis M, Ashur-Fabian O. Thyroid hormone regulates adhesion, migration and matrix metalloproteinase 9 activity via αvβ3 integrin in myeloma cells. Oncotarget. 2014;5(15):6312–22.
19. Cuénot L. Anatomie, éthologie et systématique des échinodermes. Traité de Zoologie. 1948;11:3–275.
20. Custodio MR, Imsiecke G, Borojevic R, Rinkevich B, Rogerson A, Müller WE. Evolution of cell adhesion systems: evidence for Arg-Gly-Asp-mediated adhesion in the protozoan Neoparamoeba aestuarina. J Eukaryot Microbiol. 1995;42(6):721–4. https://doi.org/10.1111/j.1550-7408.1995.tb01623.x.
21. Czarkwiani A, Dylus DV, Oliveri P. Expression of skeletogenic genes during arm regeneration in the brittle star Amphiura filiformis. Gene Expr Patterns. 2013;13(8):464–72. https://doi.org/10.1016/j.gep.2013.09.002.
22. Das B, Matsuda H, Fujimoto K, Sun G, Matsuura K, Shi Y-B. Molecular and genetic studies suggest that thyroid hormone receptor is both necessary and sufficient to mediate the developmental effects of thyroid hormone. Gen Comp Endocrinol. 2010;168(2):174–80. https://doi.org/10.1016/j.ygcen.2010.01.019.
23. Davidson EH, Rast JP, Oliveri P, Ransick A, Calestani C, Yuh C-H, Minokawa T, Amore G, Hinman V, Arenas-Mena C, Otim O, Brown CT, Livi CB, Lee PY, Revilla R, Rust AG, Jun Pan Z, Schilstra MJ, Clarke PJC, Bolouri H. A genomic regulatory network for development. Science. 2002;295(5560):1669–78. https://doi.org/10.1126/science.1069883.
24. Davis PJ, Davis FB, Lin H-Y, Mousa SA, Zhou M, Luidens MK. Translational implications of nongenomic actions of thyroid hormone initiated at its integrin receptor. Am J Physiol-Endocrinol Metabol. 2009;297(6):E1238–46. https://doi.org/10.1152/ajpendo.00480.2009.
25. Davis PJ, Goglia F, Leonard JL. Nongenomic actions of thyroid hormone. Nat Rev Endocrinol. 2016;12(2):111–21. https://doi.org/10.1038/nrendo.2015.205.
26. Davis PJ, Mousa SA, Lin H-Y. Nongenomic actions of thyroid hormone: the integrin component. Physiol Rev. 2021;101(1):319–52. https://doi.org/10.1152/physrev.00038.2019.
27. Dubois P. The skeleton of postmetamorphic echinoderms in a changing world. Biol Bull. 2014;226(3):223–36. https://doi.org/10.1086/BBLv226n3p223.
28. Dylus DV, Czarkwiani A, Stångberg J, Ortega-Martinez O, Dupont S, Oliveri P. Large-scale gene expression study in the ophiuroid Amphiura filiformis provides insights into evolution of gene regulatory networks. EvoDevo. 2016;7(1):2. https://doi.org/10.1186/s13227-015-0039-x.
29. Eales JG. Iodine metabolism and thyroid-related functions in organisms lacking thyroid follicles: are thyroid hormones also vitamins? Proceedings of the society for experimental biology and medicine. Soc Exp Biol Med. 1997;214(4):302–17.
30. Edmiston J, Farmer M, Pitt-Rivers R, Ramsden DB, Rioch F. Thyroxine in plants. Sci Progress. 1993;77(1/2):131–8.
31. Eliceiri BP, Cheresh DA. The role of αv integrins during angiogenesis. Mol Med. 1998;4(12):741–50. https://doi.org/10.1007/BF03401768.
32. Erkenbrack EM, Thompson JR. Cell type phylogenetics informs the evolutionary origin of echinoderm larval skeletogenic cell identity. Commun Biol. 2019. https://doi.org/10.1038/s42003-019-0417-3.
33. Evans RM, Mangelsdorf DJ. Nuclear receptors, RXR, and the Big Bang. Cell. 2014;157(1):255–66. https://doi.org/10.1016/j.cell.2014.03.012.
34. Fernandez-Serra M, Consales C, Livigni A, Arnone MI. Role of the ERK-mediated signaling pathway in mesenchyme formation and differentiation in the sea urchin embryo. Dev Biol. 2004;268(2):384–402. https://doi.org/10.1016/j.ydbio.2003.12.029.
35. Fuchs B, Wang W, Graspeuntner S, Li Y, Insua S, Herbst E-M, Dirksen P, Böhm A-M, Hemmrich G, Sommer F, Domazet-Lošo T, Klostermeier UC, Anton-Erxleben F, Rosenstiel P, Bosch TCG, Khalturin K. Regulation of polyp-to-jellyfish transition in Aurelia Aurita. Curr Biol. 2014;24(3):263–73. https://doi.org/10.1016/j.cub.2013.12.003.
36. Fukazawa H, Hirai H, Hori H, Roberts RD, Nukaya H, Ishida H, Tsuji K. Induction of abalone larval metamorphosis by thyroid hormones. Fish Sci. 2001;67(5):985–8. https://doi.org/10.2331/fishsci.67.985.
37. Gao F, Davidson EH. Transfer of a large gene regulatory apparatus to a new developmental address in echinoid evolution. Proc Natl Acad Sci. 2008;105(16):6091–6. https://doi.org/10.1073/pnas.0801201105.
38. Goldberg WM. Chemical changes accompanying maturation of the connective tissue skeletons of gorgonian and antipatharian corals. Mar Biol. 1978;49(3):203–10. https://doi.org/10.1007/BF00391132.
39. Hall BL, Thummel CS. The RXR homolog ultraspiracle is an essential component of the Drosophila ecdysone receptor. Development (Cambridge, England). 1998;125(23):4709–17. https://doi.org/10.1242/dev.125.23.4709.
40. Hertzler PL, McClay DR. αSU2, an epithelial integrin that binds laminin in the sea urchin embryo. Dev Biol. 1999;207(1):1–13. https://doi.org/10.1006/dbio.1998.9165.
41. Heyland A, Hodin J. A detailed staging scheme for late larval development in Strongylocentrotus purpuratus focused on readily-visible juvenile structures within the rudiment. BMC Dev Biol. 2014;14(1):22. https://doi.org/10.1186/1471-213X-14-22.
42. Heyland A, Moroz LL. Cross-kingdom hormonal signaling: An insight from thyroid hormone functions in marine larvae. J Exp Biol. 2005;208(23):4355–61. https://doi.org/10.1242/jeb.01877.
43. Heyland A, Price DA, Bodnarova-Buganova M, Moroz LL. Thyroid hormone metabolism and peroxidase function in two non-chordate animals. J Exp Zool Part B Mol Develop Evolut. 2006;306(6):551–66. https://doi.org/10.1002/jez.b.21113.
44. Heyland A, Reitzel AM, Hodin J. Thyroid hormones determine developmental mode in sand dollars (Echinodermata: Echinoidea). Evol Dev. 2004;6(6):382–92. https://doi.org/10.1111/j.1525-142X.2004.04047.x.
45. Hodin J, Heyland A, Mercier A, Pernet B, Cohen DL, Hamel J-F, Allen JD, McAlister JS, Byrne M, Cisternas P, George SB. Culturing echinoderm larvae through metamorphosis. Methods Cell Biol. 2019;150:125–69. https://doi.org/10.1016/bs.mcb.2018.11.004.
46. Hodin J, Hoffman JR, Miner BG, Davidson BJ. Thyroxine and the evolution oflecithotrophic development in cchinoids. Echinoderms 2000: Proceedings of the 10th International Conference, Dunedin, 447. 2001. https://books.google.ca/books?hl=en&lr=&id=NEog_WHJ5HcC&oi=fnd&pg=PA447&dq=Thyroxine+and+the+evolution+of+lecithotrophic+development+in+echinoids&ots=QOZuQi9LdQ&sig=thRD7azTmuKHyJZSCXThKQWVbrs. Accessed 31 Jan–4 Feb 2000.
47. Holzer G. Origin of thyroid hormone signalling in metazoans and implications in their metamorphosis [PhD Thesis]. Ecole normale supérieure de lyon-ENS LYON. 2015.
48. Holzer G, Roux N, Laudet V. Evolution of ligands, receptors and metabolizing enzymes of thyroid signaling. Mol Cell Endocrinol. 2017;459:5–13. https://doi.org/10.1016/j.mce.2017.03.021.
49. Huang W, Xu F, Qu T, Zhang R, Li L, Que H, Zhang G. Identification of thyroid hormones and functional characterization of thyroid hormone receptor in the pacific oyster crassostrea gigas provide insight into evolution of the thyroid hormone system. PLoS ONE. 2015;10(12):e0144991. https://doi.org/10.1371/journal.pone.0144991.
50. Incerpi S, Hsieh M-T, Lin H-Y, Cheng G-Y, De Vito P, Fiore AM, Ahmed RG, Salvia R, Candelotti E, Leone S, Luly P, Pedersen JZ, Davis FB, Davis PJ. Thyroid hormone inhibition in L6 myoblasts of IGF-I-mediated glucose uptake and proliferation: new roles for integrin αvβ3. Am J Physiol Cell Physiol. 2014;307(2):C150-161. https://doi.org/10.1152/ajpcell.00308.2013.
51. Isaeva VV, Rozhnov SV. Transformation of the ancestral body plan and axial growth in echinoderms: ontogenetic and paleontological data. Paleontol J. 2022;56(8):863–86. https://doi.org/10.1134/S0031030122080032.
52. James Cao H, Lin H-Y, Luidens MK, Davis FB, Davis PJ. Cytoplasm-to-nucleus shuttling of thyroid hormone receptor-β1 (Trβ1) is directed from A plasma membrane integrin receptor by thyroid hormone. Endocr Res. 2009;34(1–2):31–42. https://doi.org/10.1080/07435800902911810.

53. Johnson LG. Stage-dependent thyroxine effects on sea urchin development. NZ J Mar Freshwat Res. 1998;32(4):531–6. https://doi.org/10.1080/00288330.1998.9516841.
54. Johnson LG, Cartwright CM. Thyroxine-accelerated larval development in the crown-of-thorns starfish, Acanthaster planci. Biol Bull. 1996;190(3):299–301. https://doi.org/10.2307/1543021.
55. Katow H. Mechanisms of the epithelial-to-mesenchymal transition in sea urchin embryos. Tissue Barriers. 2015;3(4):e1059004. https://doi.org/10.1080/21688370.2015.1059004.
56. Khor JM, Ettensohn CA. Functional divergence of paralogous transcription factors supported the evolution of biomineralization in echinoderms. Elife. 2017;6:e32728. https://doi.org/10.7554/eLife.32728.
57. Kingsley RJ, Corcoran ML, Krider KL, Kriechbaum KL. Thyroxine and vitamin D in the gorgonian Leptogorgia virgulata. Comp Biochem Physiol A Mol Integr Physiol. 2001;129(4):897–907. https://doi.org/10.1016/S1095-6433(01)00354-3.
58. Klootwijk W, Friesema ECH, Visser TJ. A nonselenoprotein from amphioxus deiodinates triac but not T3: is triac the primordial bioactive thyroid hormone? Endocrinology. 2011;152(8):3259–67. https://doi.org/10.1210/en.2010-1408.
59. Koga H, Fujitani H, Morino Y, Miyamoto N, Tsuchimoto J, Shibata TF, Nozawa M, Shigenobu S, Ogura A, Tachibana K, Kiyomoto M, Amemiya S, Wada H. Experimental approach reveals the role of alx1 in the evolution of the echinoderm larval skeleton. PLoS ONE. 2016;11(2):e0149067. https://doi.org/10.1371/journal.pone.0149067.
60. Koga H, Matsubara M, Fujitani H, Miyamoto N, Komatsu M, Kiyomoto M, Akasaka K, Wada H. Functional evolution of Ets in echinoderms with focus on the evolution of echinoderm larval skeletons. Dev Genes Evol. 2010;220(3–4):107–15. https://doi.org/10.1007/s00427-010-0333-5.
61. Kong D, Liu Y, Zuo R, Li J. DnBP-induced thyroid disrupting activities in GH3 cells via integrin αvβ3 and ERK1/2 activation. Chemosphere. 2018;212:1058–66. https://doi.org/10.1016/j.chemosphere.2018.09.007.
62. Laudet V. The origins and evolution of vertebrate metamorphosis. Curr Biol. 2011;21(18):R726–37. https://doi.org/10.1016/j.cub.2011.07.030.
63. Li J, Liu H, Li N, Wang J, Song L. TDCPP mimics thyroid hormones associated with the activation of integrin αvβ3 and ERK1/2. Chemosphere. 2020;256:127066. https://doi.org/10.1016/j.chemosphere.2020.127066.
64. Livingston BT, Killian CE, Wilt F, Cameron A, Landrum MJ, Ermolaeva O, Sapojnikov V, Maglott DR, Buchanan AM, Ettensohn CA. A genome-wide analysis of biomineralization-related proteins in the sea urchin Strongylocentrotus purpuratus. Dev Biol. 2006;300(1):335–48. https://doi.org/10.1016/j.ydbio.2006.07.047.
65. Longabaugh WJR. BioTapestry: a tool to visualize the dynamic properties of gene regulatory networks. In: Deplancke B, Gheldof N, editors. Gene regulatory networks. Totowa: Humana Press; 2012. p. 359–94.
66. Ludwig BS, Kessler H, Kossatz S, Reuning U. RGD-binding integrins revisited: how recently discovered functions and novel synthetic ligands (re-) shape an ever-evolving field. Cancers. 2021;13(7):1711.
67. Magie CR, Martindale MQ. Cell-cell adhesion in the Cnidaria: insights into the evolution of tissue morphogenesis. Biol Bull. 2008;214(3):218–32. https://doi.org/10.2307/25470665.
68. Mann K, Wilt FH, Poustka AJ. Proteomic analysis of sea urchin (Strongylocentrotus purpuratus) spicule matrix. Proteome Sci. 2010;8:33. https://doi.org/10.1186/1477-5956-8-33.
69. Marsden M, Burke RD. Cloning and characterization of novel beta integrin subunits from a sea urchin. Dev Biol. 1997;181:234–45.
70. McCauley BS, Wright EP, Exner C, Kitazawa C, Hinman VF. Development of an embryonic skeletogenic mesenchyme lineage in a sea cucumber reveals the trajectory of change for the evolution of novel structures in echinoderms. EvoDevo. 2012;3(1):17. https://doi.org/10.1186/2041-9139-3-17.
71. McClay DR, Warner J, Martik M, Miranda E, Slota L. Gastrulation in the sea urchin. Curr Top Dev Biol. 2020;136:195–218. https://doi.org/10.1016/bs.ctdb.2019.08.004.
72. McIntyre DC, Lyons DC, Martik M, McClay DR. Branching out: Origins of the sea urchin larval skeleton in development and evolution. Genesis. 2014;52(3):173–85. https://doi.org/10.1002/dvg.22756.
73. Miller AEM, Heyland A. Endocrine interactions between plants and animals: implications of exogenous hormone sources for the evolution of hormone signaling. Gen Comp Endocrinol. 2010;166(3):455–61. https://doi.org/10.1016/j.ygcen.2009.09.016.
74. Miller AEM, Heyland A. Iodine accumulation in sea urchin larvae is dependent on peroxide. J Exp Biol. 2013;216(5):915–26. https://doi.org/10.1242/jeb.077958.
75. Mooi R, David B. Evolution within a bizarre phylum: homologies of the first echinoderms1. Am Zool. 1998;38(6):965–74. https://doi.org/10.1093/icb/38.6.965.
76. Murdock DJE. The 'biomineralization toolkit' and the origin of animal skeletons. Biol Rev. 2020;95(5):1372–92. https://doi.org/10.1111/brv.12614.
77. Nieberler M, Reuning U, Reichart F, Notni J, Wester H-J, Schwaiger M, Weinmüller M, Räder A, Steiger K, Kessler H. Exploring the role of RGD-recognizing integrins in cancer. Cancers. 2017. https://doi.org/10.3390/cancers9090116.
78. Nowak D, Florek M, Nowak J, Kwiatek W, Lekki J, Chevallier P, Hacura A, Wrzalik R, Ben-Nissan B, Van Grieken R, Kuczumow A. Morphology and the chemical make-up of the inorganic components of black corals. Mater Sci Eng C. 2009;29(3):1029–38. https://doi.org/10.1016/j.msec.2008.08.028.
79. Paris M, Escriva H, Schubert M, Brunet F, Brtko J, Ciesielski F, Roecklin D, Vivat-Hannah V, Jamin EL, Cravedi J-P, Scanlan TS, Renaud J-P, Holland ND, Laudet V. Amphioxus postembryonic development reveals the homology of chordate metamorphosis. Curr Biol. 2008;18(11):825–30. https://doi.org/10.1016/j.cub.2008.04.078.
80. Paris M, Hillenweck A, Bertrand S, Delous G, Escriva H, Zalko D, Cravedi J-P, Laudet V. Active metabolism of thyroid hormone during metamorphosis of amphioxus. Integr Comp Biol. 2010;50(1):63–74. https://doi.org/10.1093/icb/icq052.
81. Parks AL, Parr BA, Chin J-E, Leaf DS, Raff RA. Molecular analysis of heterochronic changes in the evolution of direct developing sea urchins. J Evol Biol. 1988;1(1):27–44. https://doi.org/10.1046/j.1420-9101.1988.1010027.x.
82. Phatarphekar A, Buss JM, Rokita SE. Iodotyrosine deiodinase: a unique flavoprotein present in organisms of diverse phyla. Mol Bio Syst. 2013;10(1):86–92. https://doi.org/10.1039/C3MB70398C.
83. Pia TS, Johnson T, George SB. Salinity-induced morphological changes in Pisaster ochraceus (Echinodermata: Asteroidea) larvae. J Plankton Res. 2012;34(7):590–601. https://doi.org/10.1093/plankt/fbs032.
84. Pisani D, Feuda R, Peterson KJ, Smith AB. Resolving phylogenetic signal from noise when divergence is rapid: a new look at the old problem of echinoderm class relationships. Mol Phylogenet Evol. 2012;62(1):27–34. https://doi.org/10.1016/j.ympev.2011.08.028.
85. Rafiq K, Shashikant T, McManus CJ, Ettensohn CA. Genome-wide analysis of the skeletogenic gene regulatory network of sea urchins. Development. 2014;141(4):950–61. https://doi.org/10.1242/dev.105585.
86. Reich A, Dunn C, Akasaka K, Wessel G. Phylogenomic analyses of Echinodermata support the sister groups of Asterozoa and Echinozoa. PLoS ONE. 2015;10(3):e0119627. https://doi.org/10.1371/journal.pone.0119627.
87. Roche J. Biochimie comparée des scléroprotéines iodées des Anthozoaires et des Spongiaires. Cell Mol Life Sci. 1952;8(2):45–54.
88. Röttinger E, Besnardeau L, Lepage T. A Raf/MEK/ERK signaling pathway is required for development of the sea urchin embryo micromere lineage through phosphorylation of the transcription factor Ets. Development. 2004;131(5):1075–87. https://doi.org/10.1242/dev.01000.
89. Rulon O. The modification of developmental patterns in the sand dollar by Thiourea. Physiol Zool. 1950;23(3):248–57. https://doi.org/10.1086/physzool.23.3.30152082.
90. Sainath SB, André A, Castro LFC, Santos MM. The evolutionary road to invertebrate thyroid hormone signaling: Perspectives for endocrine disruption processes. Comp Biochem Physiol C Toxicol Pharmacol. 2019;223:124–38. https://doi.org/10.1016/j.cbpc.2019.05.014.
91. Saito M, Seki M, Amemiya S, Yamasu K, Suyemitsu T, Ishihara K. Induction of metamorphosis in the sand dollar Peronella japonica by thyroid hormones. Dev Growth Differ. 1998;40(3):307–12.
92. Saito, Minoru, Kyo Yamasu, and Takashi Suyemitsu. Binding properties of thyroxine to nuclear extract from sea urchin larvae. Zoological science. 2012;29(2):79–82.
93. Shashikant T, Khor JM, Ettensohn CA. From genome to anatomy: the architecture and evolution of the Skeletogenic gene regulatory network of Sea urchins and other echinoderms. Genesis. 2018;56(10):e23253. https://doi.org/10.1002/dvg.23253.

94. Siuda JF, DeBernardis JF. Naturally occurring halogenated organic compounds. Lloydia. 1973;36(2):107–43.
95. Smirnov AV. Paedomorphosis and heterochrony in the origin and evolution of the class holothuroidea. Paleontol J. 2015;49(14):1597–615. https://doi.org/10.1134/S003103011514018X.
96. Smirnov AV. Parallelisms in the evolution of sea cucumbers (Echinodermata: Holothuroidea). Paleontol J. 2016;50(14):1610–25. https://doi.org/10.1134/S0031030116140082.
97. Smith AB, Reich M. Tracing the evolution of the holothurian body plan through stem-group fossils. Biol J Lin Soc. 2013;109(3):670–81. https://doi.org/10.1111/bij.12073.
98. Smith MM, Cruz Smith L, Cameron RA, Urry LA. The larval stages of the sea urchin, Strongylocentrotus Purpuratus. J Morphol. 2008;269(6):713–33. https://doi.org/10.1002/jmor.10618.
99. Strathmann RR, Fenaux L, Strathmann MF. Heterochronic developmental plasticity in larval sea urchins and its implications for evolution of Nonfeeding larvae. Evolution. 1992;46(4):972–86. https://doi.org/10.1111/j.1558-5646.1992.tb00613.x.
100. Strathmann, Megumi F. Reproduction and development of marine invertebrates of the northern Pacific coast: data and methods for the study of eggs, embryos, and larvae. University of Washington Press, 1987.
101. Susan JM, Just ML, Lennarz WJ. Cloning and characterization of alphaP integrin in embryos of the sea urchin Strongylocentrotus purpuratus. Biochem Biophys Res Commun. 2000;272:929–35.
102. Tarrant AM. Endocrine-like signaling in cnidarians: current understanding and implications for ecophysiology. Integr Comp Biol. 2005;45(1):201–14. https://doi.org/10.1093/icb/45.1.201.
103. Taylor E, Heyland A. Evolution of thyroid hormone signaling in animals: non-genomic and genomic modes of action. Mol Cell Endocrinol. 2017;459:14–20. https://doi.org/10.1016/j.mce.2017.05.019.
104. Taylor E, Heyland A. Thyroid hormones accelerate initiation of skeletogenesis via MAPK (ERK1/2) in Larval Sea Urchins (Strongylocentrotus purpuratus). Front Endocrinol. 2018. https://doi.org/10.3389/fendo.2018.00439.
105. Taylor E, Heyland A. Evolution of non-genomic nuclear receptor function. Mol Cell Endocrinol. 2022;539:111468. https://doi.org/10.1016/j.mce.2021.111468.
106. Taylor E, Wynen H, Heyland A. Thyroid hormone membrane receptor binding and transcriptional regulation in the sea urchin Strongylocentrotus purpuratus. Front Endocrinol. 2023;14:1382.
107. Telford MJ, Lowe CJ, Cameron CB, Ortega-Martinez O, Aronowicz J, Oliveri P, Copley RR. Phylogenomic analysis of echinoderm class relationships supports Asterozoa. Proc Royal Soc B Biol Sci. 2014;281(1786):20140479. https://doi.org/10.1098/rspb.2014.0479.
108. Viera-Vera J, García-Arrarás JE. Molecular characterization and gene expression patterns of retinoid receptors, in normal and regenerating tissues of the sea cucumber, Holothuria glaberrima. Gene. 2018;654:23–35. https://doi.org/10.1016/j.gene.2018.01.102.
109. Wang S, Shibata Y, Tanizaki Y, Zhang H, Yan W, Fu L, Shi Y-B. Comparative analysis of transcriptome profiles reveals distinct and organ-dependent genomic and nongenomic actions of thyroid hormone in Xenopus tropicalis tadpoles. Thyroid Off J Am Thyroid Assoc. 2023;33(4):511–22. https://doi.org/10.1089/thy.2022.0469.
110. Wei Z, Angerer RC, Angerer LM. Direct development of neurons within foregut endoderm of sea urchin embryos. Proc Natl Acad Sci. 2011;108(22):9143–7. https://doi.org/10.1073/pnas.1018513108.
111. Wessel GM, Brayboy L, Fresques T, Gustafson EA, Oulhen N, Ramos I, Reich A, Swartz SZ, Yajima M, Zazueta V. The biology of the germ line in echinoderms. Mol Reprod Dev. 2014;81(8):679–711. https://doi.org/10.1002/mrd.22223.
112. Wray GA, Raff RA. Pattern and process heterochronies in the early development of sea urchins. Semin Dev Biol. 1990;1:245–51.
113. Wynen H, Taylor E, Heyland A. Thyroid hormone-induced cell death in sea urchin metamorphic development. J Expe Biol. 2022;225(23):jeb244560.
114. Yajima M. A switch in the cellular basis of skeletogenesis in late-stage sea urchin larvae. Dev Biol. 2007;307(2):272–81. https://doi.org/10.1016/j.ydbio.2007.04.050.
115. Yamakawa S, Morino Y, Honda M, Wada H. The role of retinoic acid signaling in starfish metamorphosis. EvoDevo. 2018;9(1):10. https://doi.org/10.1186/s13227-018-0098-x.
116. Yamakawa S, Morino Y, Kohtsuka H, Wada H. Retinoic acid signaling regulates the metamorphosis of feather stars (crinoidea, echinodermata): insight into the evolution of the animal life cycle. Biomolecules. 2020. https://doi.org/10.3390/biom10010037.
117. Zamora S, Rahman IA, Sumrall CD, Gibson AP, Thompson JR. Cambrian edrioasteroid reveals new mechanism for secondary reduction of the skeleton in echinoderms. Proc Royal Soc B Biol Sci. 2022;289(1970):20212733. https://doi.org/10.1098/rspb.2021.2733.
118. Zhang X, Sun L, Yuan J, Sun Y, Gao Y, Zhang L, Li S, Dai H, Hamel J-F, Liu C, Yu Y, Liu S, Lin W, Guo K, Jin S, Xu P, Storey KB, Huan P, Zhang T, Xiang J. The sea cucumber genome provides insights into morphological evolution and visceral regeneration. PLOS Biol. 2017;15(10):e2003790. https://doi.org/10.1371/journal.pbio.2003790.

Publisher's Note